

## **A cell-based assay reveals nuclear translocation of intracellular domains released by SPPL proteases**

**Torben Mentrup, Robert Häsler, Regina Fluhrer, Paul Saftig, Bernd Schröder**

### **Angaben zur Veröffentlichung / Publication details:**

Mentrup, Torben, Robert Häsler, Regina Fluhrer, Paul Saftig, and Bernd Schröder. 2015. "A cell-based assay reveals nuclear translocation of intracellular domains released by SPPL proteases." *Traffic: the international journal of intracellular transport* 16 (8): 871-92. <https://doi.org/10.1111/tra.12287>.

### **Nutzungsbedingungen / Terms of use:**

**licgercopyright**

Dieses Dokument wird unter folgenden Bedingungen zur Verfügung gestellt: / This document is made available under the following conditions:

**Deutsches Urheberrecht**

Weitere Informationen finden Sie unter: / For more information see:

<https://www.uni-augsburg.de/de/organisation/bibliothek/publizieren-zitieren-archivieren/publizieren>



# A cell-based assay reveals nuclear translocation of intracellular domains released by SPPL proteases

Running title: Nuclear translocation after intramembrane cleavage

Torben Mentrup<sup>1</sup>, Robert Häsler<sup>2</sup>, Regina Fluhrer<sup>3,4</sup>, Paul Saftig<sup>1</sup> and Bernd Schröder<sup>1\*</sup>

<sup>1</sup>Biochemical Institute, Christian Albrechts University of Kiel, Otto-Hahn-Platz 9, D-24118 Kiel, Germany

<sup>2</sup>Institute of Clinical Molecular Biology, Christian Albrechts University of Kiel, Schittenhelmstr. 12, D-24105 Kiel Kiel, Germany

<sup>3</sup>Adolf-Butenandt-Institute for Biochemistry, Ludwig Maximilians University of Munich, Feodor-Lynen-Strasse 17, D-81377 Munich, Germany

<sup>4</sup>DZNE – German Center for Neurodegenerative Diseases, Feodor-Lynen-Strasse 17, D-81377 Munich, Germany

\* Corresponding author:

Dr. Bernd Schröder, MD PhD, Biochemical Institute, Christian Albrechts University of Kiel, Otto-Hahn-Platz 9, D-24118 Kiel, Germany, Phone: +49-431-8802218; Fax: +49-431-8802238

E-mail: baschroeder@biochem.uni-kiel.de

## Synopsis

The intramembrane proteases Signal peptide peptidase-like-2a/b (SPPL) liberate intracellular domains (ICDs) from type II transmembrane proteins. We describe a cell-based assay employing  $\beta$ -galactosidase fragment complementation for quantifying activity of SPPL2 or other intramembrane proteases based on detecting nuclear translocation of released substrate ICDs. In this system we demonstrate nuclear translocation of CD74-, TNF- and ITM2B-ICDs and characterize SFRP2 as potential transcriptional target of the CD74-ICD. The assay will allow to screen for novel inhibitors and to analyze the regulation of intramembrane proteases.

## Abbreviations

The abbreviations used are:  $\beta$ Gal,  $\beta$ -galactosidase;  $\beta$ GEFC,  $\beta$ -galactosidase enzyme fragment complementation; ICD, intracellular domain; I-CLIP, intramembrane cleaving protease; ITM2B, integral membrane protein 2B; Luc, firefly luciferase; NTF, N-terminal fragment; RIP, regulated intramembrane proteolysis; SFRP2, Secreted frizzled-related protein 2; SPPL, Signal peptide peptidase-like; TMEM192, transmembrane protein 192; TNF, Tumor necrosis factor/TNF-alpha.

## Keywords

Intramembrane proteolysis; Signal-peptide-peptidase-like protease;  $\gamma$ -secretase;  $\beta$ -galactosidase; Protein fragment complementation; Nuclear translocation

## Abstract

**During Regulated Intramembrane Proteolysis (RIP) a membrane-spanning substrate protein is cleaved by an ectodomain sheddase and an intramembrane cleaving protease. A cytoplasmic intracellular domain (ICD) is liberated, that can migrate to the nucleus thereby influencing transcriptional regulation. Signal peptide peptidase-like (SPPL) 2a and 2b have been implicated in RIP of type II transmembrane proteins. Even though SPPL2a might represent a potential pharmacological target for treatment of B cell-mediated autoimmunity, no specific and potent inhibitors for this enzyme are currently available. We report here on the first quantitative cell-based assay for measurement of SPPL2a/b activity. Demonstrating the failure of standard Gal4/VP16 reporter assays for SPPL2a/b analysis, we have devised a novel system employing  $\beta$ -galactosidase ( $\beta$ Gal) complementation. This is based on detecting nuclear translocation of the**

**proteolytically released substrate ICDs which results in specific restoration of  $\beta$ Gal activity. Utilizing this potentially high-throughput compatible new setup, we demonstrate nuclear translocation of the ICDs from ITM2B, TNF and CD74 and identify SFRP2 as potential transcriptional downstream target of the CD74 ICD. We show that the presented assay is easily adaptable to other intramembrane proteases and therefore represents a valuable tool for the functional analysis and development of new inhibitors of this class of enzymes.**

Intramembrane proteolysis involves the processing of membrane-spanning substrate proteins within their hydrophobic transmembrane segments by so-called I-CLIPs (intramembrane cleaving proteases) (1). Usually, this process is part of a proteolytic cascade which is initiated by processing of the substrate's ectodomain and thereby is involved in the turnover of a variety of membrane proteins (1). Beyond that, cleavage fragments

generated by intramembrane proteolysis can be actively involved in cellular signal transduction after their release from the membrane involving translocation to the nucleus as it is the case in Notch signaling (2,3).

The SPP/SPPL family of aspartyl I-CLIPs is constituted by Signal peptide peptidase (SPP) and four homologous SPP-like (SPPL) proteins SPPL2a, -b, -c and SPPL3 which differ in their subcellular localizations (4,5). SPP/SPPL proteases show selectivity for substrate proteins in type 2 orientation and exhibit a catalytic center similar to that of the presenilins which are the catalytically active part of the  $\gamma$ -secretase complex. The family member SPPL2a is primarily localized in membranes of lysosomes and late endosomes (6) and was shown to cleave N-terminal fragments (NTF) of Tumor necrosis factor (TNF) (7,8), Fas ligand (9), ITM2B (10) and TMEM106B (11) in cell-based set-ups. So far, the invariant chain (CD74), a chaperone of the MHCII complex, represents the only *in vivo* validated substrate of this protease (12-14). CD74 binds MHCII in the ER and facilitates targeting of the complex to endosomal compartments where CD74 undergoes step-wise proteolytic degradation starting from the luminal domain (15). In B lymphocytes of SPPL2a-deficient mice, significant amounts of uncleaved CD74 NTF accumulate and disturb homeostasis of these cells. This leads to a block of B cell maturation at the transitional stage 1 (T1), a loss of dendritic cells and severely impaired humoral immune responses in *Spp12a*<sup>-/-</sup> mice (12-14). Though this phenotype is clearly driven by the CD74 NTF as documented by its alleviation in *Spp12a*<sup>-/-</sup> *Cd74*<sup>-/-</sup> mice (12), the fate and putative downstream function of the CD74 intracellular domain (ICD) that is released by SPPL2a is insufficiently resolved. In contrast to SPPL2a, SPPL2b was reported to reside primarily at the plasma membrane (5,6). Although the substrate spectra of SPPL2a and SPPL2b were found to overlap significantly in cell-based systems, SPPL2b was described to be dispensable for CD74 proteolysis under endogenous conditions indicating that both proteases exhibit distinct functions *in vivo* (5).

Based on the described immunological phenotype of *Spp12a*<sup>-/-</sup> mice (12), pharmacological inhibition of SPPL2a activity has been proposed as a strategy for depleting and/or inhibiting B cells and dendritic cells in a therapeutic context. Depletion of B cells has been shown to be beneficial in a variety of autoimmune disorders including systemic lupus erythematosus and is currently achieved with antibody-based therapeutics (16). Thus, a small molecule-based approach utilizing SPPL2a inhibitors would exhibit significant advantages. As expected from the catalytic center homology, several  $\gamma$ -secretase inhibitors, like inhibitor X, also target SPP/SPPL proteases. To date, (Z-LL)<sub>2</sub>-ketone represents the only SPP/SPPL inhibitor that spares  $\gamma$ -secretase activity but acts unselectively on several members of the SPP/SPPL protease family (4).

Since *in vitro* reconstitution of recombinantly expressed SPP/SPPL proteases as it is routinely employed for rhomboid I-CLIPs (17) has not been achieved yet, functional analysis of SPPL2

proteases relies on cell-based systems followed by Western blot determination of uncleaved or cleaved forms of substrate proteins. Thus, a sensitive, quantitative and potentially high throughput-compatible assay for monitoring activity of SPPL2a and other SPPL2 proteases is currently not available. This would, however, represent a prerequisite not only to further analyse the function and regulation of this protease but also to search for novel inhibitors and to optimize the available compounds.

For analysis of  $\gamma$ -secretase, cell-based reporter assays have been successfully employed, especially for monitoring cleavage of the amyloid precursor protein (APP) (18-21) and Notch1 (19,22). In several of these studies a reporter composed of the yeast DNA binding protein Gal4 and the transcriptional activator VP16 was fused to the cytosolic C-terminus of the  $\gamma$ -secretase substrates (18-20). Upon proteolytic release of the ICD, the Gal4/VP16 reporter induces transcription of a luciferase via a Gal4-dependent promoter from a co-transfected plasmid. Luciferase activity is determined luminometrically and normalized via activity of a co-expressed reporter enzyme.

Here, we report on a novel cell-based reporter assay system for determining the activity of SPPL2 proteases which is also applicable to other I-CLIPs. We show that conventional Gal4/VP16-based reporter systems interfere with the trafficking of type II-oriented SPPL substrate proteins preventing their use for this class of proteases. Therefore, the novel assay utilizes  $\beta$ -galactosidase ( $\beta$ gal) enzyme fragment complementation ( $\beta$ GEFC) in order to detect nuclear translocation of the intracellular domains (ICDs) released from the substrate proteins by the intramembrane cleavage. Using this system, we assessed the ability of the ICDs from individual SPPL2a and SPPL2b substrates for nuclear localization. With respect to the putative therapeutic impact of the SPPL2a substrate CD74, we specifically validated our readout system for this substrate. Furthermore, we provide first insights into transcriptional regulation exerted by the CD74 ICD.

## Results

### Conventional Gal4/VP16-assays are not applicable to SPPL2a/b substrates

Cell-based assays utilizing the Gal4/VP16 reporter system have been successfully applied to determine the activity of several I-CLIPs. We therefore tried to expand this system to SPPL2 substrates. For this purpose, murine TNF, a substrate of SPPL2a, was tagged at its cytoplasmic N-terminus with the Gal4/VP16 reporter and then transiently expressed in HeLa cells to verify the subcellular localisation of this construct by indirect immunofluorescence (Figure 1A). In comparison to a protein carrying an HA epitope tag in the same position, the Gal4/VP16-TNF fusion protein demonstrated a significantly altered subcellular distribution and was predominantly trapped in perinuclear structures not co-localizing with any organelles as demonstrated here for the Golgi marker protein GM130 (Figure

1A). Presumably, these structures represent aggregates of misfolded proteins. In addition to this, Western Blot analysis revealed rather low expression of the Gal4/VP16-tagged TNF in comparison to the HA-tagged protein (Figure 1B) and only very minor amounts of the TNF NTF which is generated by ectodomain shedding and represents the actual SPPL2a substrate were detected. Furthermore, no decrease of the TNF NTF levels was observed after co-expression of active SPPL2a. This was in sharp contrast to the HA-tagged TNF NTF, which was clearly processed by SPPL2a (Figure 1B) what could be blocked by application of the SPP/SPPL inhibitor X.

Nevertheless, we tried to employ the Gal4/VP16-tagged TNF reporter construct for a luciferase based SPPL activity assay and transfected this construct and a corresponding reporter plasmid into HeLa cells (Figure 1C). Despite the disturbed trafficking and poor expression of the fusion protein, transfection of this construct was associated with a significant increase of the Firefly/Renilla luciferase ratio as compared to vector-transfected control cells. However, this ratio could not be modulated by application of the SPP/SPPL inhibitor X. This strongly indicates that the luciferase expression induced by the Gal4/VP16 TNF reporter construct was not related to SPPL-mediated intramembrane proteolysis, but rather to unrelated processes like the ERAD pathway.

### **Large cytosolic tags interfere with correct sorting of SPPL2a/b substrates**

Since TNF could be expressed with small N-terminal tags like the HA epitope but not with the large Gal4/VP16 tag, which comprise 9 and ~230 amino acids, respectively, we wondered whether the size of a cytosolically fused reporter might also critically influence expression and subcellular sorting of other SPPL2a/b substrates. For this purpose we compared processing and trafficking of CD74 devoid of any N-terminal tag (CD74-HA) with a GFP-CD74 fusion protein (Figure 1D) since GFP is of a similar size as the Gal4/VP16 reporter. A major function of CD74 is to mediate trafficking of MHC II complexes to antigen-processing endosomal compartments, where CD74 is subjected to proteolytic degradation starting from its C-terminal luminal domain (15). As expected, CD74 was localized primarily in vesicular compartments after heterologous expression in HeLa cells. However, under the same conditions GFP-CD74 was predominantly retained in the endoplasmic reticulum as revealed by co-localization with PDI (Figure 1D). Correspondingly, SPPL2a-mediated processing of the NTFs that were produced from the GFP-tagged variant was not observed. In contrast, upon expression of CD74-HA (Figure 1E) full-length protein and different C-terminally truncated degradation intermediates were detected under steady-state conditions. As we showed previously (5,12), co-expression of SPPL2a significantly reduced the CD74 NTF (Figure 1E). Thus, both tested type II-oriented SPPL2a/b substrates TNF and CD74 do not tolerate larger tags at their short cytosolic termini in order to allow trafficking to the plasma membrane or the endocytic pathway which is a prerequisite for their proteolytic processing.

### **The $\beta$ Gal $\alpha$ -tag is compatible with correct sorting and processing of SPPL2a/b substrates**

Since these findings precluded the use of Gal4/VP16 based reporter assays for the analysis of SPPL2a/b dependent proteolysis we considered alternative approaches. Therefore, we sought for a reporter system that would only require the addition of a short tag to the N-terminus of the substrate protein which was tolerated by CD74 and TNF (Figure 1) and also other substrates like TMEM106B (11) and ITM2B (10). This essential selection criterion was fulfilled by  $\beta$ -galactosidase enzyme fragment complementation ( $\beta$ GEFC) (23,24).

We therefore devised the system illustrated in Figure 2A in order to measure the proteolytic activity of SPPL2 proteases based on determining the nuclear translocation of the released substrate ICDs. To achieve this, we aimed to express the large  $\beta$ Gal  $\omega$ -fragment, that is on its own catalytically inactive, in the nucleus of a reporter cell line. The complementing  $\beta$ Gal  $\alpha$ -peptide, that has a limited size of only  $\approx$ 50 aa and is required to restore enzymatic activity, would then be fused to the N-terminus of CD74 or other SPPL2a/b substrate proteins. Then,  $\beta$ Gal activity reconstitution could only occur after proteolytic liberation and nuclear translocation of the ICD.

To test if the  $\beta$ Gal  $\alpha$ -tag would be compatible with trafficking and proteolysis of CD74, we created an N-terminally  $\alpha$ -tagged CD74 construct ( $\alpha$ -CD74) (Figure 2B). For the case that the CD74 ICD generated by SPPL2a would not intrinsically localize to the nucleus, we generated a second construct harboring an SV40 NLS sequence ( $\alpha$ -NLS-CD74) between the  $\alpha$ -tag and the CD74 N-terminus (Figure 2B). We analyzed trafficking and proteolytic processing of these CD74 fusion proteins in comparison to wild type CD74 by indirect immunofluorescence (Figure 2C) and Western blotting (Figure 2D,E), respectively. Neither targeting to endosomal/lysosomal compartments nor processing by SPPL2a was altered by the described tags. The latter applied to co-expressed (Figure 2D) as well as endogenous SPPL proteases (Figure 2E) as revealed by the NTF stabilization induced by the SPP/SPPL inhibitors (Z-LL)<sub>2</sub>-ketone and inhibitor X. These findings strongly support the applicability of  $\beta$ GEFC to monitor intramembrane cleavage of CD74.

### **$\beta$ GEFC can be employed to detect nuclear localisation**

Based on a previous report (25), we generated a reporter construct ( $\omega_{nuc}$ ) of the  $\beta$ Gal  $\omega$ -fragment fused C-terminally to three SV40 nuclear localization sequences (NLS), a nuclear retention sequence from SC35 (NRS) and an additional NLS from c-Myc (Figure 3A). Using this construct, we produced a stable HEK293T  $\omega_{nuc}$  reporter cell line that showed homogenous nuclear expression of the  $\omega$ -fragment (Figure 3A). As a positive control for the devised assay, we employed a GFP carrying the  $\beta$ Gal  $\alpha$ -tag in addition to three NLS at its N-terminus ( $\alpha$ -eGFP<sub>nuc</sub>) in order to facilitate constitutive transport of the expressed protein to the nucleus which was confirmed by fluorescence microscopy

(Figure 3B). In contrast, TMEM192 is a multi-spanning integral protein of the lysosomal membrane (26,27) for which proteolytic cleavage has not been observed, thus precluding that the N-terminally fused  $\alpha$ -tag reaches the  $\omega$ -reporter in the nucleus (Figure 3C). The  $\alpha$ -eGFP<sub>nuc</sub> and  $\alpha$ -TMEM192 control constructs were transiently expressed in the  $\omega$ <sub>nuc</sub>-reporter cell line and  $\beta$ Gal activity was determined using a luminescent substrate (Figure 3D). In order to account for differences in transfection efficiency, the  $\beta$ Gal activity was normalized to the activity of a co-expressed firefly luciferase. Whereas significant  $\beta$ Gal activity was detected in cells expressing the nuclear-localized  $\alpha$ -eGFP<sub>nuc</sub>, almost no  $\beta$ Gal reconstitution was observed following expression of  $\alpha$ -TMEM192. This confirms suitability of the described system to determine nuclear translocation of  $\alpha$ -tagged proteins.

### **The CD74 ICD is capable of nuclear translocation**

To verify the applicability of the developed  $\beta$ GEFC based assay system we focused on CD74 as model substrate. Therefore we first transfected the  $\alpha$ -CD74 and  $\alpha$ -NLS-CD74 constructs described in Figure 2 into the  $\omega$ <sub>nuc</sub> reporter cell line and analyzed the cells for  $\beta$ Gal complementation. Upon application of these constructs to our  $\beta$ Gal assay system, we observed a normalized  $\beta$ Gal activity that was significantly higher than that of the negative control  $\alpha$ -TMEM192 (Figure 4A). This detected  $\beta$ Gal activity indicated a translocation of the CD74 ICD to the nucleus following its processing. This effect was further enhanced by an additional NLS sequence. Nevertheless, these data strongly indicate the capability of the  $\alpha$ -tagged CD74 ICD to translocate to the nucleus upon its generation by SPPL2a. We also confirmed dose dependency of the  $\beta$ Gal activity resulting from transfection of  $\alpha$ -CD74 (Figure 4B).

In the following, we focused on the  $\alpha$ -tagged CD74 wild type construct ( $\alpha$ -CD74) to validate that the  $\beta$ Gal reconstitution following expression of this construct was indeed dependent on intramembrane proteolysis by SPPL2a that precedes nuclear translocation of the CD74 N-terminus. Therefore, we co-expressed  $\alpha$ -CD74 with SPPL2a and observed that presence of the protease significantly augmented  $\beta$ Gal activity (Figure 4C) indicating increased levels of CD74 ICD in the nucleus in the presence of SPPL2a. This effect was reversed when activity of SPPL2a was blocked by concomitant inhibitor X application, an inhibitor of SPP/SPPL proteases and  $\gamma$ -secretase. These findings are in agreement with observations from Western blot analysis (Figure 2D), where co-expression of SPPL2a enhanced turnover of CD74 NTF.

We also investigated processing of  $\alpha$ -tagged CD74 by endogenous proteases in this system using inhibitor treatment (Figure 4D). The SPPL2a inhibitors (Z-LL)<sub>2</sub>-ketone and inhibitor X significantly reduced  $\alpha$ -CD74 associated  $\beta$ Gal reconstitution. Processing of the CD74 luminal domain represents a prerequisite of CD74 intramembrane cleavage by SPPL2a (12) since only the NTF and not the full-length protein is a substrate of the protease. We evaluated the effect of

preventing lysosomal/endosomal acidification by bafilomycin A1 and of endosomal protease inhibition by E64 or leupeptin on CD74 ICD generation in the  $\beta$ Gal system. Both approaches are known to inhibit CD74 degradation (28,29). Here, all three compounds reduced the detected normalized  $\beta$ Gal activity in  $\alpha$ -CD74 expressing cells versus solvent-treated controls indicating that upon interference with CD74 ectodomain proteolysis less CD74 ICD is produced. This agrees well with the observation that co-expressed SPPL2a does not modulate the full-length form of CD74, but only a truncated NTF (Figure 2D) as shown by Western blotting. Since (Z-LL)<sub>2</sub>-ketone and inhibitor X are active against several members of the SPP/SPPL protease family, we sought to confirm the role of endogenous SPPL2a for CD74 ICD release in our  $\beta$ Gal reporter cell line by knockdown of SPPL2a. In cells treated with SPPL2a versus non-targeting control siRNA (Figure 4E), normalized  $\beta$ Gal reporter activity following  $\alpha$ -CD74 transfection was reduced to a similar degree as by treatment with (Z-LL)<sub>2</sub>-ketone or inhibitor X (Figure 4D). This result validates the described reporter assay as a suitable readout for SPPL2a activity.

### **The CD74 ICD is degraded by the proteasome**

We wanted to elucidate the pathways involved in turnover of this proteolytic fragment following its release by SPPL2a. Therefore, we treated  $\alpha$ -CD74 transfected  $\omega$ <sub>nuc</sub> cells with the proteasome inhibitors epoxomicin and bortezomib or a mixture of amastatin, bestatin and AAF-CMK, all inhibitors of cytosolic peptidases. Incubation with the proteasome inhibitors led to a significant increase in normalized  $\beta$ Gal activity, whereas treatment with the peptidase inhibitor did not show any significant effect under these conditions (Figure 5A). We scrutinized if the observed effect upon proteasomal inhibition indeed reflected stabilization of the CD74 ICD generated by SPPL2a-mediated intramembrane cleavage. Therefore, we treated the cells with inhibitor X for 2 h before and also during epoxomicin application. The interference with CD74 processing resulted in a significant, however not complete, rescue of the epoxomicin dependent increase in  $\beta$ Gal reconstitution (Figure 5B). Furthermore, we excluded by Western blot analysis that significant stabilization of the  $\beta$ Gal  $\omega$ <sub>nuc</sub> reporter had been induced by the applied proteasomal inhibitors (Figure 5C). Though this does not rule out additional stabilising effects of the proteasome inhibitor on CD74 fragments generated by putative SPPL2a-independent mechanisms such as ER-associated degradation (ERAD) due to overexpression, these results nonetheless indicate a major role of the proteasome in the degradation of the CD74 ICD.

### **A potential role of the CD74 ICD in transcriptional regulation**

After having documented the capability of the  $\alpha$ -CD74 ICD to translocate to the nucleus, we sought to investigate any putative impact of the CD74 ICD on transcriptional regulation. Since direct

overexpression of the CD74 ICD has not been successful in our hands, presumably due to its small size, we devised the system depicted in Figure 5D for controlled overexpression of the CD74 ICD mimicking its proteolytic release from a transmembrane precursor. In the generated constructs (Figure 5D), the 35 N-terminal residues of murine CD74 (ICD) were fused to eGFP followed by the transmembrane segment of human syntaxin 7 anchoring the fusion protein to the membrane. Between the CD74 ICD and the eGFP, a linker was inserted containing either a cleavage site (ENLYFQG) for the Nla protease from the tobacco etch virus (TEV protease) or a stretch of alanines ( $\pm$  TEV site). In both constructs, TEV protease is co-expressed from the same plasmid employing an internal ribosome entry site (IRES) mediating release of the CD74 ICD specifically from the fusion protein with the TEV cleavage site whereas the CD74 ICD remains membrane-bound in the control. Since the TEV protease is highly specific, heterologous expression of this protease is well tolerated in different experimental systems, including mammalian cells (30).

We generated stable HEK293 cells inducibly expressing both constructs and validated their functionality regarding membrane localization of the CD74 ICD-GFP fusion proteins (not shown) and the proteolytic processing upon presence of the TEV cleavage site (Figure 5E). Interestingly, the released CD74 ICD was not directly observed (not shown) despite its confirmed production indicating that intrinsic properties of this fragment impede its Western blot-based detection. We determined and compared genome wide transcriptome profiles of both cell lines. In order to detect changes in gene expression patterns induced by the proteolytically released CD74 ICD, we calculated fold changes between the cell line expressing the cleavable CD74 ICD fusion protein versus the control cell line where the ICD is not liberated. Transcripts that appeared differentially expressed more than two-fold between the two cell lines are listed in Suppl. Table S1. Among these were ten protein-coding transcripts, from which four appeared to be up- and six down-regulated. We did not further analyze *OR514A*, *TASR30* and *KRTAP9-1* due to their very specific roles as olfactory and taste receptors or in hair follicles, respectively. In contrast, the suggested differential expression of *TULP3*, *ZNF763*, *SFRP2*, *DHRX*, *LUM*, *TPTE* and *CNTN1* was re-evaluated by quantitative RT-PCR (Suppl. Figure S1). In this analysis, *ZNF763* mRNA was not detected and no difference was found for *TPTE*, *TULP3* and *DHRX*. However, CD74 ICD-associated upregulation of *SFRP2* (Figure 5F) as well the reduction of *CNTN1* and *LUM* expression was confirmed.

We asked if this effect of the overexpressed CD74 ICD could also be relevant under endogenous conditions. *Sfrp2* mRNA has been detected in bone marrow-derived dendritic cells (BMDC) by transcriptomic profiling (31). Since dendritic cells abundantly express endogenous CD74, we analyzed consequences of a reduced ICD generation in BMDCs. Therefore, we compared *Sfrp2* transcript levels in *Spp12a*<sup>-/-</sup> and *Cd74*<sup>-/-</sup> BMDCs, in which generation of the CD74 ICD cannot occur due to the absence of either the

protease or the substrate, to BMDCs isolated from wild type mice (Figure 5G). *SFRP2* expression was significantly down-regulated in both the *SPPL2a*- and the *CD74*-deficient cells. This agrees well to the described increase of *SFRP2* expression upon *CD74* ICD overexpression. In conclusion, these findings strongly indicate that the *CD74* ICD can have a regulatory impact on gene expression also under endogenous conditions advocating further investigations especially regarding the underlying mechanism.

### **Nuclear translocation of ICDs from other SPPL2a/b substrates**

Following the corroboration of the  $\beta$ Gal assay system to monitor intramembrane cleavage of *CD74* proteolysis, we sought to evaluate its applicability to other substrates of SPPL proteases. Therefore, we created N-terminally  $\alpha$ -tagged expression constructs of *TNF* and *ITM2B* (Figure 6A) with or without an inserted additional NLS sequence. We analyzed the subcellular distribution of these  $\alpha$ -tagged proteins in comparison to the wild type proteins with an N-terminal HA tag (Figure 6B). In analogy to *CD74*, we did not detect any impact of the  $\alpha$ -tag on intracellular trafficking of *TNF* and *ITM2B*. Both constructs were able to reach the cell surface. Expression of the generated *TNF* and *ITM2B* constructs ( $\alpha$ -*TNF*,  $\alpha$ -*ITM2B*) resulted in normalized  $\beta$ Gal activities that were significantly higher than those provoked by the negative control  $\alpha$ -*TMEM192* (Figure 6C). Similar to *CD74*,  $\beta$ Gal reconstitution was enhanced by an additional NLS in the *TNF* and *ITM2B* reporter constructs ( $\alpha$ -NLS-*TNF*,  $\alpha$ -NLS-*ITM2B*).

We aimed to confirm that the  $\alpha$ -*TNF* and  $\alpha$ -*ITM2B* induced assay signals were dependent on intramembrane cleavage by *SPPL2a* and/or *SPPL2b*. Therefore, we co-expressed  $\alpha$ -*TNF* and  $\alpha$ -*ITM2B* with both proteases (Figure 6D,E) and observed enhanced  $\alpha$ -*TNF* and  $\alpha$ -*ITM2B* associated  $\beta$ Gal reconstitution what could be partially blocked by concomitant application of inhibitor X. In conclusion, these results show that the described assay can also be employed to determine the turnover of other substrates than *CD74* by SPPL proteases. Furthermore, our findings demonstrate that in this system *SPPL2a/b*-generated *TNF* and *ITM2B* ICDs are able to translocate to the nucleus. While this has been suggested before for the *TNF* ICD (7,32), a capability of the *ITM2B* ICD to access the nucleus has not been reported previously according to our knowledge.

### **The $\beta$ Gal reporter assay can be adapted to other intramembrane proteases**

Finally, we wanted to assess if the described  $\beta$ Gal reporter assay system can be adapted to substrate proteins of different topology and/or of other than SPPL intramembrane proteases. To investigate this, we chose the type 1 transmembrane protein *Notch* as one of the best studied substrates of intramembrane proteolysis (3). Ligand binding induces proteolytic shedding of the *Notch* ectodomain that is followed by  $\gamma$ -secretase processing of the remaining C-terminal stub enabling well-documented nuclear translocation of

the ICD (3). We used a Notch expression construct devoid of the ectodomain (Notch $\Delta$ E) (Figure 7A) (33). Therefore, upon expression in HeLa cells this truncated Notch protein was constitutively processed by  $\gamma$ -secretase and the released C-terminal ICD could be detected in the nucleus (Figure 7B). Upon inhibition of  $\gamma$ -secretase by DAPT, generation of the ICD was prevented so that the Notch $\Delta$ E protein remained membrane-associated (Figure 7B). With respect to applicability in our reporter assay, the employed Notch $\Delta$ E construct carried the  $\beta$ Gal  $\alpha$ -tag at its cytosolic C-terminus. In the  $\omega_{\text{nuc}}$  reporter cell line, expression of the Notch $\Delta$ E- $\alpha$  construct restored  $\beta$ Gal activity to about 70% of the level observed with the positive control  $\alpha$ -eGFP $_{\text{nuc}}$  (Figure 7C). Upon concomitant  $\gamma$ -secretase inhibition by DAPT, significantly less  $\beta$ Gal activity was measured. This effect was not observed with the SPP/SPPL inhibitor (Z-LL) $_2$ -ketone. Thus, the established  $\beta$ Gal reporter assay can be employed to monitor  $\gamma$ -secretase mediated cleavage of Notch as well as the nuclear translocation of the Notch ICD. This finding substantiates applicability of the system to monitor proteolysis of different substrate topologies as well as by other classes of intramembrane proteases.

## Discussion

In this study, we sought to create a cell-based reporter assay to monitor the activity of the intramembrane proteases SPPL2a and SPPL2b in order to provide an alternative to cumbersome Western blot procedure when studying these enzymes. To achieve this, we failed to adapt the Gal4/VP16 reporter system that has been successfully applied to monitor cleavage by  $\gamma$ -secretase (18-22) or the ER protease SPP (34,35). Apparently, in these studies the cleavage of type 1 transmembrane proteins or ER proteins in type 2 orientation was analyzed. Here, we showed that N-terminal fusion of the Gal4/VP16 reporter, that comprises about 230 amino acids, or a protein of a similar size (GFP) was not compatible with regular trafficking and proteolysis of the SPPL2a/b substrates TNF and CD74. These proteins exhibit a type 2 transmembrane topology with a short cytoplasmic N-terminal domain (~30 residues) and need to travel via the secretory pathway to the plasma membrane and/or endosomal compartments. In the case of CD74, essential sorting motifs in this N-terminal part of the protein have been identified (36). The Gal4/VP16-TNF construct was expressed at very low levels as compared to the wild type construct suggesting, that in this case even folding and/or membrane insertion of the fusion protein in the ER were disturbed. Since the other currently known SPPL2a/b substrates ITM2B (10), Fas ligand (9), transferrin receptor (37) and TMEM106 (11) exhibit a similar topological layout to the ones examined, it can be concluded that the Gal4/VP16 reporter system is not suitable to monitor intramembrane cleavage by SPPL2a/b.

We demonstrate here that a split reporter system based on  $\beta$ Gal ( $\beta$ GEFC), that only requires the addition of a short tag to the N-terminus of the substrate protein, can be exploited to create a cell-

based reporter assay for SPPL2a/b-mediated intramembrane proteolysis. This system allowed quantitative detection of the ICDs following their release from the membrane-bound substrate proteins. We showed that modulation of protease activity in a positive or negative way by overexpression, knockdown or pharmacological inhibition, respectively, was reflected in a corresponding modulation of the assay signal thus validating this as a quantitative readout of SPPL2a/b-mediated proteolysis. We especially sought to provide an assay for the intramembrane cleavage of CD74 by SPPL2a based on the documented *in vivo* relevance of this process and its potential as a therapeutic target (12-14). However, we also confirmed applicability of the  $\beta$ GEFC-based assay system for other SPPL2a/b substrates like TNF and ITM2B and demonstrated that cleavage of the type 1 transmembrane protein Notch1 by  $\gamma$ -secretase could be monitored by this means. Thus, the  $\beta$ GEFC reporter assay is not restricted to a certain substrate topology and may be further extended to other classes of intramembrane proteases.

Protein fragment complementation describes the reconstitution of a protein's function or enzymatic activity from two separately synthesized fragments when these are brought into proximity (38). A variety of different split-reporter systems have been designed and used in multiple applications, especially for the analysis of protein-protein interactions (38). Among these, a quite unique property of split  $\beta$ Gal is the pronounced size asymmetry of the two fragments comprising ~50 ( $\alpha$ ) and ~950 ( $\omega$ ) amino acids (23) that are capable of reconstituting  $\beta$ Gal activity, making it especially suited for the purpose of this study. We found that the small  $\beta$ Gal  $\alpha$ -peptide in contrast to other reporters did not interfere with trafficking and proteolysis of SPPL2a/b substrates.  $\beta$ Gal-based readout systems have been successfully employed in high-throughput screening applications (39). Similar to other split-protein reporters,  $\beta$ GEFC has been exploited to monitor protein-protein interactions (40). However, due to the high affinity complementation of the two  $\beta$ Gal fragments already their presence in the same subcellular compartment can be sufficient to promote assembly of a functional enzyme. This fact has been utilized for designing cell-based assays to detect nuclear translocation of target proteins (24,25,41), especially in order to provide a readout for the activation of certain signaling pathways, like Wnt (41) and glucocorticoid receptor (25) signalling. In the present study we have extended this application to monitor proteolytic processes at biological membranes by the proteases SPPL2a/b. Adaption of the described system to design assays for other intramembrane proteases is possible and may provide essential advantages over previously employed reporters especially for substrate proteins with short cytoplasmic domains.

We demonstrated that the  $\beta$ GEFC assay system is suitable to monitor SPPL2a-mediated cleavage of CD74 since interference with this process led to a significant reduction of the assay signal. However, pharmacological inhibition of SPPL2a activity only blocked about 30% of the

signal. Similar effects were observed upon knockdown of the protease which led to a significant, though incomplete depletion of the SPPL2a protein. Therefore, we hypothesize that also in the inhibitor-treated cells residual SPPL2a activity accounts for the remaining assay signal. This would indicate that either the affinity of the used compounds or their cell-permeability or a combination of both are limiting in order to achieve a full inhibition. However, we can also not exclude that part of the CD74-associated assay signal reflects SPPL2a-independent degradative routes that liberate CD74 proteolytic fragments into the cytosol. Furthermore, also minor amounts of the  $\beta$ Gal  $\omega$ -fragment in the cytosol, that we failed to detect with immunofluorescence, could in principle account for a SPPL2a-independent background signal. However, this should have also affected signals for the negative control  $\alpha$ -TMEM192, which we used as baseline. Therefore, we consider this as unlikely.

When studying intramembrane proteolysis, the fate and function of the intracellular cleavage products is an immanent question related to the technical difficulties to detect these often small, low-abundant protein fragments biochemically. The latter also applies to the ICD released from CD74. We have been unable to detect this released CD74 ICD by biochemical means directly in total cell lysates what is most likely due to its small size of 30-40 amino acids and/or its rapid turnover. Our assay data (Figure 5) point to a degradation of the CD74 ICD by the proteasome. This pathway might be influenced by the putative D box motif (RXXL) in the cytoplasmic region of the CD74 protein (42). However, also concurrent inhibition of the proteasome (bortezomib, epoximicin) did not enhance biochemical detectability of this cleavage product by Western blotting in our hands. This may indicate that primarily its unfavourable properties impair its recovery with this technique which was not resolved despite significant optimization efforts. In this context, the described  $\beta$ GEFC assay system represents a valuable approach to examine the cell biological fate of the CD74 ICD. Beyond providing a quantitative readout for protease activity it also allows to explore the capability of the respective cleavage fragments for entering the nucleus. Nuclear translocation of CD74 fragments has been suggested before (43), however, the proteolytic machinery for the intramembrane cleavage of CD74 was unknown until recently (12-14). In our  $\beta$ GEFC system, we could demonstrate that the CD74 ICD released by the intramembrane protease SPPL2a has the capability to migrate to the nucleus which could indicate a physiological function of this process similar to other I-CLIP substrates (44).

In this regard, we demonstrated that the CD74 ICD may play a role in influencing transcriptional regulation as exemplified by the identification of *SFRP2* as a potential target gene. In different cellular systems, modulation of CD74 ICD generation and release was reflected in corresponding changes of *SFRP2* transcript levels. *SFRP2* is a secretory protein that has been found to be a negative regulator of Wnt signaling (45,46). Furthermore, amongst other functions *SFRP2* has been suggested to act as a tumor suppressor since it was shown to induce apoptosis and promote

tumorigenesis (46,47). The physiological relevance of a regulatory circuit between CD74 and *SFRP2* in dendritic cells as we showed here needs further insights. Interestingly, *SFRP2* was reported to be secreted in pathophysiologically relevant amounts by multiple myeloma, a neoplasm of plasma cells (48). This process was demonstrated to contribute to the bone loss induced by these tumors via suppressing bone formation. At the same time, high expression levels of CD74 are usually observed in multiple myeloma (49). It may be interesting to test if the CD74 ICD contributes to the documented up-regulation of *SFRP2* in these neoplastic plasma cells. The precise molecular mechanism how the CD74 ICD enhances *SFRP2* expression is currently unclear. It has been reported previously that the released CD74 ICD has an impact on NF $\kappa$ B signaling (42). Therefore, we analyzed our microarray data set for any CD74 ICD-associated expression modulation of established NF $\kappa$ B target genes or components of this pathway (Suppl. Table S2). However, we could not find any changes arguing for a differential activation of the NF $\kappa$ B pathway in those cells expressing the cleavable versus the non-cleavable CD74 ICD fusion protein. This was also supported by biochemical analysis of I $\kappa$ B $\alpha$  levels (not shown). Therefore, we did not obtain any evidence that in this cell system the effect on *SFRP2* involves components of the NF $\kappa$ B pathway. We think that the overexpression system we have utilized to mimic proteolytic liberation of the CD74 ICD in combination with transcriptomic profiling represents a well-controlled, unbiased approach that will also be useful to investigate the effects of other ICDs released by I-CLIPs. In this context, we consider the current dataset merely as a proof-principle experiment that provides first indications for a regulatory role of the CD74 ICD. We think that our findings strongly advocates to adapt the system to (murine) immune cells that also endogenously express CD74 which would further enhance the validity of the approach.

Using the  $\beta$ GEFC assay, we could also confirm nuclear translocation of the TNF ICD in line with previous reports (7,32). This ICD was reported to enhance expression of the pro-inflammatory IL12 after its liberation by SPPL2a/b-mediated proteolysis (7). In contrast to TNF, the molecular function of the ITM2B protein is much less understood to date (50). This protein is genetically linked to the familial British and Danish forms of dementia and has been reported to influence processing of the amyloid precursor protein (51). However, little is known about the physiological relevance of the ITM2B intramembrane cleavage by SPPL2a/b following release of the ectodomain by ADAM10 (10). Here, we reveal for the first time that the ITM2B ICD can travel to the nucleus following its proteolytic liberation. This could suggest a specific function of the ITM2B ICD in signal transduction and transcriptional regulation that will need to be further investigated.

Another interesting question is whether the relative small ICD of this protein as well as that of TNF and CD74 is trafficked to the nucleus by specific transport mechanisms. Since molecules with a size <40 kDa are able to enter this compartment by passive diffusion (52,53), this most

likely also applies to the small substrate ICDs. In general, our findings on the capability of SPPL2a/b substrates to localize to the nucleus are in agreement with findings for many of the numerous substrates of the related  $\gamma$ -secretase complex (44). For those substrates of  $\gamma$ -secretase or other intramembrane proteases where biochemical detection of the intracellular cleavage products is inherently difficult the described  $\beta$ GEFC reporter system will provide a powerful tool to clarify the cellular fates of these fragments. In addition to this, the assay described above will provide a versatile technique not only for elaborating intramembrane cleavage of RIP substrates but also for the preceding and kinetically linked shedding process as we could show for the luminal processing of CD74. Therefore, we are confident that the devised assay system provides a new valuable tool for the functional analysis of SPPL2a/b and also other intramembrane proteases as well as for the search of novel inhibitors of these enzymes.

## Materials and Methods

### Reagents

The SPP/SPPL-inhibitors (Z-LL)<sub>2</sub>-ketone (Peptanova) and inhibitor X (EMD Millipore) were used at final concentrations of 20  $\mu$ M and 1  $\mu$ M, respectively. For selective inhibition of  $\gamma$ -secretase, DAPT (Sigma) was applied at 1  $\mu$ M final concentration. Proteasome inhibition was performed with bortezomib (Selleck chemicals) and epoxomicin (Peptanova) at concentrations of 5  $\mu$ g/ml and 1  $\mu$ M, respectively. Amastatin (1  $\mu$ M, Peptanova), bestatin (20  $\mu$ M, Sigma) and AAF-CMK (10  $\mu$ M, Peptanova) were used to target cytosolic peptidases. To interfere with processing of the CD74 luminal domain, leupeptin (2.5  $\mu$ M, Roth), E64 (10  $\mu$ M, Enzo) and bafilomycin A1 (300 nM, Sigma) were utilized as inhibitors of lysosomal proteases and lysosomal acidification, respectively. Except for AAF-CMK, leupeptin and E64 which were dissolved in H<sub>2</sub>O, stock solutions from all other compounds were prepared in DMSO (Roth) or DMSO/H<sub>2</sub>O mixtures. Doxycyclin (used at 10  $\mu$ g/ml) was purchased from Sigma.

### Cloning and constructs

Murine TNF was tagged with an N-terminal HA- and a C-terminal V5 tag and inserted into the pcDNA3.1 hygro (+) vector backbone (Invitrogen). An N-terminal HA-tag was added to the open reading frame of murine ITM2B via PCR using extended primers and the fusion construct was cloned into pcDNA3.1 hygro (+) via its XbaI and BamHI sites. For generation of the Gal4/VP16-mTNF fusion construct the Gal4/VP16 reporter coding was amplified from pMst-GV (18) and fused to mTNF via fusion PCR. The pL8G5-Luc vector, the response plasmid for the Gal4/VP16 reporter, as well as the pMst-GV plasmid were a kind gift of Thomas Sūdohf and Jacqueline Burré. The pRL-TK vector coding for a Renilla Luciferase used as transfection control for Gal4/VP16 assays was from Promega. To furthermore test the applicability of large tags to the N-termini of SPPL2a/b substrate molecules, the p31

isoform of murine CD74 (12) CD74 was cloned into pEGFP-C1 (Clontech) to fuse its coding sequence with the one of GFP.

The nuclear  $\beta$ Gal reporter construct ( $\omega_{nuc}$ ) was cloned by deletion of the coding sequence for amino acids 12-42 of *E. coli*  $\beta$ Gal. To achieve stable nuclear localization of the  $\beta$ Gal reporter, three SV40 nuclear localization sequences (NLS, DPKKKRKV) (54), the SC35 nuclear retention signal (NRS, PPPVSKRESKRSRSKSPPKSPEEEGAVSSDLKVRKAA, see (55)) and an additional NLS derived from the transcription factor c-Myc (DLKVRKAA) (56) were fused by two consecutive PCRs to the 3' end of the reporter construct according to (25). The final PCR product was inserted via appended BamHI and XbaI sites into pcDNA3.1 hygro+ that was also used for all expression constructs described below. The resulting construct was termed  $\omega_{nuc}$ . For each SPPL substrate analyzed, expression constructs with the complementing  $\beta$ Gal  $\alpha$ -peptide fused to the N-terminus ( $\alpha$ -tag) were generated with or without an additional SV40 NLS in order to facilitate nuclear translocation of the released ICD also in the absence of a functional intrinsic nuclear import motif. In a first step, either the  $\alpha$ -tag alone (MSSNSLAVVLQRRDWENP GVTQLNRLAHPPFASWRNSEEARTDRPSQQLRS LNGE) or in combination with an additional SV40 NLS was appended to the 5' end of the coding sequence of the p31 isoform of murine CD74 (12) by PCR with an BamHI site in between. The whole fragment was then integrated via introduced NheI and XbaI sites into pcDNA3.1 hygro+. For the generation of murine TNF and ITM2B assay constructs, the CD74 coding sequence was excised from the  $\alpha$ -tagged CD74 constructs by restriction digest with BamHI and XbaI and the respective open reading frames were inserted in frame via corresponding 5' and 3'-terminal sites added by PCR. A C-terminally  $\alpha$ -tagged expression construct of the established  $\gamma$ -secretase substrate Notch1 was generated based on the murine Notch $\Delta$ E-GFP construct described in (33). This was devoid of the Notch1 extracellular domain allowing constitutive cleavage by  $\gamma$ -secretase independent of ligand binding and ectodomain shedding. To enable detection of this construct, an HA-tag was inserted between the Notch $\Delta$ E coding sequence and the  $\beta$ Gal  $\alpha$ -tag. As a positive control for nuclear localization, we fused the  $\beta$ Gal  $\alpha$ -tag and three SV40 NLS to the open reading frame of GFP (from peGFP-N1, Clontech) resulting in a constitutive nuclear transport of GFP ( $\alpha$ -eGFP<sub>nuc</sub>). As an extranuclear negative control, we created an N-terminally  $\alpha$ -tagged construct of the human lysosomal integral transmembrane protein 192 ( $\alpha$ -TMEM192) that we have characterized previously (26,27). Plasmids coding for murine SPPL2a/b and the inactive SPPL2a-D416A mutant have been described before (5,6,12). An expression construct of firefly luciferase in a pcDNA3 vector (57) was obtained from Addgene (plasmid no. 18964).

To generate a system that allowed for expression of the CD74 ICD (aa 1-35) a construct was generated that harboured this protein fragment attached to a GFP and a human syntaxin 7 membrane anchor (aa 229-261). Either a TEV protease cleavage site (ENLYFQG) or a stretch of 7

alanines (A<sub>7</sub>) were inserted between the CD74 ICD and the membrane anchored GFP to allow or inhibit cleavage by a myc-tagged TEV protease coexpressed from the same plasmid via an IRES sequence. While the CD74 ICD coding sequence was amplified from plasmids described above, the nucleotide sequences corresponding to GFP was amplified from pEGFP-N1 (Clontech). The coding sequence of the human syntaxin7 membrane anchor as well as the TEV protease cleavage site or the A<sub>7</sub> stretch were attached by consecutive PCRs using extended primers. IRES sequence and the TEV protease open reading frame were amplified from pIRES2-EGFP (Clontech) or pRK1043 (Addgene 8835), respectively. Finally, the sequences were joined by overlap-extension PCRs and cloned into pcDNA5.1/FRT/TO (Life Technologies) via its BamHI and XhoI sites. The constructs were termed CD74 ICD-TEV-GFP<sub>mem</sub> or CD74-ICD-A<sub>7</sub>-GFP<sub>mem</sub>, respectively.

### Cell culture and transfection

HeLa (DSMZ) and HEK293T cells were maintained in DMEM (Sigma) supplemented with 10% fetal bovine serum (Biochrom) as well as 100 U/ml penicillin (Sigma) and 100 µg/ml Streptomycin (Sigma). Cells were cultivated at 37°C in a humidified 5% CO<sub>2</sub>/95% air atmosphere. All transfections of plasmid DNA were performed with Turbofect (Thermo Scientific) according to manufacturer's instructions.

A reporter cell line stably expressing ω<sub>nuc</sub> was generated by transfection of HEK293T cells with the corresponding plasmid and subsequent selection of positive clones with 250 µg/ml hygromycin (Invivogen). After subcloning, individual clones were evaluated regarding homogeneity of expression and nuclear localization of the reporter construct as determined by indirect immunofluorescence as well as discrimination between positive and negative control under assay conditions. The best-performing cell line according to these criteria was chosen for further experiments and termed ω<sub>nuc</sub>.

To generate a cell line that would allow for the inducible expression of the CD74 ICD, the FlpIn<sup>TM</sup>-Rex<sup>TM</sup>293 cell line (Life Technologies) was transfected with either the CD74 ICD-TEV-GFP<sub>mem</sub> or CD74-ICD-A<sub>7</sub>-GFP<sub>mem</sub> construct and the pOG44 vector (Life Technologies). Subsequently, cells were selected with 100 µg/ml hygromycin and 10 µg/ml blasticidin (Invivogen). Since the FlpIn<sup>TM</sup> system facilitates site-directed integration of the transfected constructs and transgene expression in the selected cells was homogenous as determined by indirect immunofluorescence, cells were maintained as a batch without subcloning. In the following, these CD74 ICD-TEV-GFP<sub>mem</sub> or CD74 ICD-A<sub>7</sub>-GFP<sub>mem</sub> cell lines were used for microarray and qRT-PCR analysis.

For knock-down of *SPPL2A* in the HEK293T reporter cell line, a pool of four gene-specific siRNAs (SMARTpool: GUUGUUGCCUGGA GACGUA, GGAGUGGACUAGUUGAAU, CCUCAUGCCUGUUCAAUA, GGUAACAGCUA UCAGAUGA) as well as of non-targeting siRNAs (pool #1) were obtained from Thermo Scientific and transfected using INTERFERin (Polyplus

transfection) following the supplier's recommendations. A final concentration of 20 nM siRNA in the culture medium was used for efficient knockdown of *SPPL2A*. siRNA transfection was directly performed at the time of cell seeding and repeated after 48 h incubation.

### Gal4/VP16-transactivation assays

HeLa cells (5x10<sup>4</sup>) were seeded in 24-well-plates and transfected with pRL-TK, pL8G5-Luc and empty vector or Gal4/VP16-TNF as indicated. On the next day, the cells were treated with 1 µM inhibitor X or the corresponding amount of DMSO for 6 h and lysed by applying Passive lysis buffer (Promega). Afterwards, 20 µl of the uncleared lysate were analyzed for luciferase activity using the Dual-Luciferase<sup>®</sup> Reporter Assay System kit (Promega) according to the manufacturer's instructions. Luminescent signals were detected using a GloMax<sup>™</sup> 96 well plate luminometer (Promega) applying a two-injections-protocol. For evaluation of the experiments, the determined Firefly luciferase activity was divided by the corresponding Renilla activity for each sample. This Firefly/Renilla luciferase signal ratio was then normalized to that from the substrate-expressing, solvent treated sample.

### βGFC assay procedure

For βGal enzyme fragment complementation assays, 10<sup>4</sup> cells of the ω<sub>nuc</sub> reporter cell line were seeded in 100 µl medium without hygromycin in 96 well plates (Greiner Bio-One) suitable for luminescence assays. On the following day, cells were transfected with α-tagged substrate or control constructs as well as firefly luciferase to allow normalization of transfection efficiency. After one day of culture post transfection, cells were either used directly for luminescent determination of βGal and luciferase activities or following a 6 h treatment with inhibitors as indicated. Activities of the reporter enzymes were measured employing the Dual-Light<sup>®</sup> Luciferase & β-Galactosidase Reporter Gene Assay System (Life technologies) and a GloMax<sup>™</sup> 96 well plate luminometer E6521 (Promega). Measurements were performed at least in technical duplicates based on two independent transfections. For evaluation, βGal/firefly luciferase (βGal/Luc) activity ratios were calculated for each individual sample. These ratios were normalized as indicated either to positive control samples (α-eGFP<sub>nuc</sub>) that were part of each assay or, when protease activity was modulated, to solvent treated or mock transfected samples. In both cases, the individual sample ratios were divided by the mean value of the respective control samples that were used as basis for the normalization. Figures show mean values and SEM of at least three independent experiments each carried out with at least two technical duplicates per condition.

### Western blotting

Protein was extracted from harvested cells as described previously (26). Protein concentration of total lysates was determined with a BCA protein assay (bicinchoninic acid, Thermo Scientific). Following electrophoretic separation by SDS-PAGE

with tris-glycine (58) or tris-tricine (59) buffer systems as applicable, semi-dry transfer of protein to nitrocellulose membranes was performed as reported in (26). For immunodetection of murine CD74, the established monoclonal antibody In-1 directed against the CD74 intracellular domain was employed (BD Biosciences). To detect cleavage fragments of TNF a rabbit polyclonal antibody was generated against a synthetic peptide corresponding to aa 4-22 of murine TNF (ESMIRDVELAEEALPQKMG). A rabbit monoclonal anti-GFP antibody was obtained from Cell signaling. The monoclonal 3F10 antibody recognizing the Hemagglutinin (HA) epitope and the monoclonal 9B11 antibody against the Myc epitope were purchased from Roche and Cell Signaling, respectively. The generation of antibodies against murine and human SPPL2a has been reported before (6,60). Expression of the  $\beta$ Gal  $\omega$ -fragment was detected using an anti- $\beta$ Gal-antibody (Promega). To confirm equal protein loading, a rabbit polyclonal antibody against  $\beta$ -Actin (Sigma) was used. HRP-conjugated secondary antibodies for chemiluminescent detection were from Dianova.

### Indirect immunofluorescence

For indirect immunofluorescence analysis,  $5 \times 10^4$  HeLa cells were seeded out on coverslips in 12 well plates the day before transfection. One day post transfection cells were fixed with 4% (w/v) paraformaldehyde and permeabilized with 0.2% (w/v) saponine, both in PBS, according to the protocol described earlier (26). Employed primary antibodies included anti-LAMP2 (2D5) (61), anti-GM130 (BD Biosciences) and anti-PDI (Abcam) as well as the already mentioned anti-CD74, anti- $\beta$ Gal, anti-TNF Nterm and anti-HA. For visualization, Alexa-488 and -594 coupled secondary antibodies were utilized (MobiTec). After mounting in Mowiol supplemented with DABCO (1,4-diazobicyclo-(2.2.2) octane) and DAPI (4-,6-diamidino-2-phenylindole) photographs from optical sections were acquired with a FV1000 confocal laser scanning microscope (Olympus) equipped with an U Plan S Apo 64x oil immersion objective and Olympus Fluoview Software (3.0a). Adobe Photoshop was applied for further processing.

### Microarray

To evaluate potential transcriptional effects due to liberation of the overexpressed CD74 ICD, an exemplary microarray experiment was carried out using the CD74 ICD-TEV-GFP<sub>mem</sub> and CD74-ICD-A7-GFP<sub>mem</sub> cell lines described above as well as a corresponding stably empty vector transfected cell line. In order to induce expression of the CD74 ICD fusion proteins, cells were treated for 24h with 10  $\mu$ g/ml doxycyclin (Sigma). Subsequently, RNA was isolated using the Nucleospin RNA<sup>®</sup> kit (Macherey Nagel). Genome wide transcriptome profiles were generated employing Human Gene 2.0 ST Arrays (Affymetrix) according to the manufacturer's guidelines and further processed as previously described (62), while transcripts with a fold change > 2.0 or < -2.0 were considered as differentially expressed.

### Generation of BMDCs

SPPL2a- and CD74 deficient mice were described before (12,63). For differentiation of bone marrow derived dendritic cells (BMDC) according to (64) the bone marrow of 3 animals per genotype was prepared by flushing tibia and femur bone marrow using 10 ml BMDC medium consisting of RPMI medium (GIBCO) supplied with 10% FBS, 100 U/ml penicillin, 100  $\mu$ g/ml streptomycin and 50  $\mu$ M  $\beta$ -mercaptoethanol (GIBCO).  $5 \times 10^6$  bone marrow cells were seeded in 10 cm dishes in 10 ml of RPMI medium supplied with 20 ng/ml GM-CSF (Immunotools). Fresh medium (10 ml) supplemented with the same amount of GM-CSF was added after 3 days. At day 6, 10 ml of medium were replaced by fresh BMDC medium containing 10 ng/ml GM-CSF. At day 7,  $1.5 \times 10^6$  cells were seeded and harvested for RNA extraction at the following day.

### Quantitative RT-PCR

RNA was extracted using the Nucleospin RNA<sup>®</sup> kit according to the manufacturer's recommendations. Afterwards, 1  $\mu$ g RNA was transcribed into cDNA using the RevertAid First Strand cDNA Synthesis Kit (Thermo Scientific) in a 20  $\mu$ l volume using random hexamer oligonucleotides. Finally 0.5  $\mu$ l cDNA per reaction were analyzed via quantitative real-time PCR using the Universal Probe Library System (Roche) and a Lightcycler 480II (Roche). The following primers were used to determine expression of Secreted frizzled-related protein 2 (*SFRP2*) and alpha tubulin for normalization:

hSFRP2-fw,	GCTAGCAGCGACC
ACCTC;	hSFRP2-rv, TTTTTCAGGCTTCACATA
CC;	hTuba1c-fw, CCCCTCAAGTTCTAGTCATGC;
hTuba1c-rv,	GCATTGCCAATCTGGACAC;
mSFRP2-fw,	AAACCCCTTTGTAAAAATGACTTCG;
mSFRP2-rv,	CAGCTTGTAATGGTCTTGCTC;
mTuba1a-fw,	CTGGAACCCACGGTCATC;
mTuba1a-rv,	GTGGCCACGAGCATAGTTATT.

Expression of murine and human *SFRP2* was normalized to mTuba1a or hTuba1c, respectively.

### Statistical analysis

Data shown represent means  $\pm$  standard error of the mean (SEM). For statistical analyses, unpaired two-tailed t-test or one-way ANOVA followed by Tukey post hoc testing were used as indicated. Significance levels of  $p < 0.05$  (\*),  $p < 0.01$  (\*\*) and  $p < 0.001$  (\*\*\*) were applied.

### Acknowledgements

We thank Dr. William Kaelin, Harvard Medical School, for providing a firefly luciferase expression construct via Addgene, Dr. David Waugh, National Cancer Institute, Rockville, for a plasmid coding for TEV protease made accessible via Addgene and Dr. Christoph Kaether, Leibniz Institute for Age Research, Jena, Germany, for the Notch $\Delta E$  construct. Furthermore, we thank Jacqueline Burré and Thomas Südhof, Stanford School of Medicine, for plasmids for the Gal4/VP16 reporter assay. We are grateful for excellent technical assistance from Sebastian Held. This work was supported by the

Deutsche Forschungsgemeinschaft as part of the SFB877 (project B7, to B.S.) and the Cluster of Excellence "Inflammation at Interfaces" as well as grant SCHR 1284/1-1 (to B.S.).

## References

1. Wolfe MS and Kopan R. Intramembrane proteolysis: theme and variations. *Science* 2004;305:1119-23.
2. Urban S and Freeman M. Intramembrane proteolysis controls diverse signalling pathways throughout evolution. *Curr Opin Genet Dev* 2002;12:512-8.
3. De Strooper B, Annaert W, Cupers P, Saftig P, Craessaerts K, Mumm JS, Schroeter EH, Schrijvers V, Wolfe MS, Ray WJ, Goate A, Kopan R. A presenilin-1-dependent gamma-secretase-like protease mediates release of Notch intracellular domain. *Nature* 1999;398:518-22.
4. Voss M, Schröder B, Flührer R. Mechanism, specificity, and physiology of signal peptide peptidase (SPP) and SPP-like proteases. *Biochim Biophys Acta* 2013;1828:2828-39.
5. Schneppenheim J, Hüttl S, Mentrup T, Lüllmann-Rauch R, Rothaug M, Engelke M, Dittmann K, Dressel R, Araki M, Araki K, Wienands J, Flührer R, Saftig P, Schröder B. The intramembrane proteases signal Peptide peptidase-like 2a and 2b have distinct functions in vivo. *Mol Cell Biol* 2014;34:1398-411.
6. Behnke J, Schneppenheim J, Koch-Nolte F, Haag F, Saftig P, Schröder B. Signal-peptide-peptidase-like 2a (SPPL2a) is targeted to lysosomes/late endosomes by a tyrosine motif in its C-terminal tail. *FEBS Lett* 2011;585:2951-7.
7. Friedmann E, Hauben E, Maylandt K, Schleege S, Vreugde S, Lichtenthaler SF, Kuhn PH, Stauffer D, Rovelli G, Martoglio B. SPPL2a and SPPL2b promote intramembrane proteolysis of TNFalpha in activated dendritic cells to trigger IL-12 production. *Nat Cell Biol* 2006;8:843-8.
8. Flührer R, Grammer G, Israel L, Condrón MM, Haffner C, Friedmann E, Bohland C, Imhof A, Martoglio B, Teplow DB, Haass C. A gamma-secretase-like intramembrane cleavage of TNFalpha by the GxGD aspartyl protease SPPL2b. *Nat Cell Biol* 2006;8:894-6.
9. Kirkin V, Cahuzac N, Guardiola-Serrano F, Huault S, Luckerath K, Friedmann E, Novac N, Wels WS, Martoglio B, Hueber AO, Zornig M. The Fas ligand intracellular domain is released by ADAM10 and SPPL2a cleavage in T-cells. *Cell Death Differ* 2007;14:1678-87.
10. Martin L, Flührer R, Reiss K, Kremmer E, Saftig P, Haass C. Regulated intramembrane proteolysis of Bri2 (Itn2b) by ADAM10 and SPPL2a/SPPL2b. *J Biol Chem* 2008;283:1644-52.
11. Brady OA, Zhou X, Hu F. Regulated Intramembrane Proteolysis of the Frontotemporal Lobar Degeneration Risk Factor, TMEM106B, by Signal Peptide Peptidase-like 2a (SPPL2a). *J Biol Chem* 2014;289:19670-80.
12. Schneppenheim J, Dressel R, Hüttl S, Lüllmann-Rauch R, Engelke M, Dittmann K, Wienands J, Eskelinen EL, Hermans-Borgmeyer I, Flührer R, Saftig P, Schröder B. The intramembrane protease SPPL2a promotes B cell development and controls endosomal traffic by cleavage of the invariant chain. *J Exp Med* 2013;210:41-58.
13. Beisner DR, Langerak P, Parker AE, Dahlberg C, Otero FJ, Sutton SE, Poirot L, Barnes W, Young MA, Niessen S, Wiltshire T, Bodendorf U, Martoglio B, Cravatt B, Cooke MP. The intramembrane protease Sppl2a is required for B cell and DC development and survival via cleavage of the invariant chain. *J Exp Med* 2013;210:23-30.
14. Bergmann H, Yabas M, Short A, Miosge L, Barthel N, Teh CE, Roots CM, Bull KR, Jeelall Y, Horikawa K, Whittle B, Balakishnan B, Sjollem G, Bertram EM, MacKay F, Rimmer AJ, Cornall RJ, Field MA, Andrews TD, Goodnow CC, Enders A. B cell survival, surface BCR and BAFFR expression, CD74 metabolism, and CD8-dendritic cells require the intramembrane endopeptidase SPPL2A. *J Exp Med* 2013;210:31-40.
15. Neeffjes J, Jongsma ML, Paul P, Bakke O. Towards a systems understanding of MHC class I and MHC class II antigen presentation. *Nat Rev Immunol* 2011;11:823-36.
16. Townsend MJ, Monroe JG, Chan AC. B-cell targeted therapies in human autoimmune diseases: an updated perspective. *Immunol Rev* 2010;237:264-83.
17. Dickey SW, Baker RP, Cho S, Urban S. Proteolysis inside the membrane is a rate-governed reaction not driven by substrate affinity. *Cell* 2013;155:1270-81.
18. Biederer T, Cao X, Sudhof TC, Liu X. Regulation of APP-dependent transcription complexes by Mint/X11s: differential functions of Mint isoforms. *J Neurosci* 2002;22:7340-51.
19. Karlstrom H, Bergman A, Lendahl U, Naslund J, Lundkvist J. A sensitive and quantitative assay for measuring cleavage of presenilin substrates. *J Biol Chem* 2002;277:6763-6.
20. Bakshi P, Liao YF, Gao J, Ni J, Stein R, Yeh LA, Wolfe MS. A high-throughput screen to identify inhibitors of amyloid beta-protein precursor processing. *J Biomol Screen* 2005;10:1-12.
21. Florean C, Zampese E, Zanese M, Brunello L, Ichas F, De GF, Pizzo P. High content analysis of gamma-secretase activity reveals variable dominance of

- presenilin mutations linked to familial Alzheimer's disease. *Biochim Biophys Acta* 2008;1783:1551-60.
22. Li J, Fici GJ, Mao CA, Myers RL, Shuang R, Donoho GP, Pauley AM, Himes CS, Qin W, Kola I, Merchant KM, Nye JS. Positive and negative regulation of the gamma-secretase activity by nicastrin in a murine model. *J Biol Chem* 2003;278:33445-9.
  23. Langley KE, Villarejo MR, Fowler AV, Zamenhof PJ, Zabin I. Molecular basis of beta-galactosidase alpha-complementation. *Proc Natl Acad Sci U S A* 1975;72:1254-7.
  24. Wehrman TS, Casipit CL, Gewertz NM, Blau HM. Enzymatic detection of protein translocation. *Nat Methods* 2005;2:521-7.
  25. Fung P, Peng K, Kobel P, Dotimas H, Kauffman L, Olson K, Eglen RM. A homogeneous cell-based assay to measure nuclear translocation using beta-galactosidase enzyme fragment complementation. *Assay Drug Dev Technol* 2006;4:263-72.
  26. Schröder B, Wrocklage C, Hasilik A, Saftig P. Molecular characterisation of 'transmembrane protein 192' (TMEM192), a novel protein of the lysosomal membrane. *Biol Chem* 2010;391:695-704.
  27. Behnke J, Eskelinen EL, Saftig P, Schröder B. Two dileucine motifs mediate late endosomal/lysosomal targeting of transmembrane protein 192 (TMEM192) and a C-terminal cysteine residue is responsible for disulfide bond formation in TMEM192 homodimers. *Biochem J* 2011;434:219-31.
  28. Landsverk OJ, Ottesen AH, Berg-Larsen A, Appel S, Bakke O. Differential regulation of MHC II and invariant chain expression during maturation of monocyte-derived dendritic cells. *J Leukoc Biol* 2012;91:729-37.
  29. Landsverk OJ, Barois N, Gregers TF, Bakke O. Invariant chain increases the half-life of MHC II by delaying endosomal maturation. *Immunol Cell Biol* 2011;89:619-29.
  30. Wehr MC, Laage R, Bolz U, Fischer TM, Grunewald S, Scheek S, Bach A, Nave KA, Rossner MJ. Monitoring regulated protein-protein interactions using split TEV. *Nat Methods* 2006;3:985-93.
  31. Pletinckx K, Stijlemans B, Pavlovic V, Laube R, Brandl C, Kneitz S, Beschin A, De BP, Lutz MB. Similar inflammatory DC maturation signatures induced by TNF or *Trypanosoma brucei* antigens instruct default Th2-cell responses. *Eur J Immunol* 2011;41:3479-94.
  32. Domonkos A, Udvardy A, Laszlo L, Nagy T, Duda E. Receptor-like properties of the 26 kDa transmembrane form of TNF. *Eur Cytokine Netw* 2001;12:411-9.
  33. Huenniger K, Kramer A, Soom M, Chang I, Kohler M, Depping R, Kehlenbach RH, Kaether C. Notch1 signaling is mediated by importins alpha 3, 4, and 7. *Cell Mol Life Sci* 2010;67:3187-96.
  34. Nyborg AC, Jansen K, Ladd TB, Fauq A, Golde TE. A signal peptide peptidase (SPP) reporter activity assay based on the cleavage of type II membrane protein substrates provides further evidence for an inverted orientation of the SPP active site relative to presenilin. *J Biol Chem* 2004;279:43148-56.
  35. Dev KK, Chatterjee S, Osinde M, Stauffer D, Morgan H, Kobialko M, Dengler U, Rueeger H, Martoglio B, Rovelli G. Signal peptide peptidase dependent cleavage of type II transmembrane substrates releases intracellular and extracellular signals. *Eur J Pharmacol* 2006;540:10-7.
  36. Bonifacino JS and Traub LM. Signals for sorting of transmembrane proteins to endosomes and lysosomes. *Annu Rev Biochem* 2003;72:395-447.
  37. Zahn C, Kaup M, Fluhrer R, Fuchs H. The transferrin receptor-1 membrane stub undergoes intramembrane proteolysis by signal peptide peptidase-like 2b. *FEBS J* 2013;280:1653-63.
  38. Michnick SW, Ear PH, Manderson EN, Remy I, Stefan E. Universal strategies in research and drug discovery based on protein-fragment complementation assays. *Nat Rev Drug Discov* 2007;6:569-82.
  39. Olson KR and Eglen RM. Beta galactosidase complementation: a cell-based luminescent assay platform for drug discovery. *Assay Drug Dev Technol* 2007;5:137-44.
  40. Rossi F, Charlton CA, Blau HM. Monitoring protein-protein interactions in intact eukaryotic cells by beta-galactosidase complementation. *Proc Natl Acad Sci U S A* 1997;94:8405-10.
  41. Verkaar F, Blankesteyn WM, Smits JF, Zaman GJ. beta-Galactosidase enzyme fragment complementation for the measurement of Wnt/beta-catenin signaling. *FASEB J* 2010;24:1205-17.
  42. Matza D, Kerem A, Medvedovsky H, Lantner F, Shachar I. Invariant chain-induced B cell differentiation requires intramembrane proteolytic release of the cytosolic domain. *Immunity* 2002;17:549-60.
  43. Becker-Herman S, Arie G, Medvedovsky H, Kerem A, Shachar I. CD74 is a member of the regulated intramembrane proteolysis-processed protein family. *Mol Biol Cell* 2005;16:5061-9.
  44. Haapasalo A and Kovacs DM. The many substrates of presenilin/gamma-secretase. *J Alzheimers Dis* 2011;25:3-28.
  45. Mii Y and Taira M. Secreted Wnt "inhibitors" are not just inhibitors: regulation of extracellular Wnt by secreted Frizzled-related proteins. *Dev Growth Differ* 2011;53:911-23.
  46. Esteve P and Bovolenta P. The advantages and disadvantages of sfrp1

- and sfrp2 expression in pathological events. *Tohoku J Exp Med* 2010;221:11-7.
47. Lee JL, Lin CT, Chueh LL, Chang CJ. Autocrine/paracrine secreted Frizzled-related protein 2 induces cellular resistance to apoptosis: a possible mechanism of mammary tumorigenesis. *J Biol Chem* 2004;279:14602-9.
  48. Oshima T, Abe M, Asano J, Hara T, Kitazoe K, Sekimoto E, Tanaka Y, Shibata H, Hashimoto T, Ozaki S, Kido S, Inoue D, Matsumoto T. Myeloma cells suppress bone formation by secreting a soluble Wnt inhibitor, sFRP-2. *Blood* 2005;106:3160-5.
  49. Stein R, Mattes MJ, Cardillo TM, Hansen HJ, Chang CH, Burton J, Govindan S, Goldenberg DM. CD74: a new candidate target for the immunotherapy of B-cell neoplasms. *Clin Cancer Res* 2007;13:5556s-63s.
  50. Del CM and Teunissen CE. Role of BRI2 in dementia. *J Alzheimers Dis* 2014;40:481-94.
  51. Matsuda S, Giliberto L, Matsuda Y, Davies P, McGowan E, Pickford F, Ghiso J, Frangione B, D'Adamio L. The familial dementia BRI2 gene binds the Alzheimer gene amyloid-beta precursor protein and inhibits amyloid-beta production. *J Biol Chem* 2005;280:28912-6.
  52. McLane LM and Corbett AH. Nuclear localization signals and human disease. *IUBMB Life* 2009;61:697-706.
  53. Paine PL, Moore LC, Horowitz SB. Nuclear envelope permeability. *Nature* 1975;254:109-14.
  54. Kalderon D, Roberts BL, Richardson WD, Smith AE. A short amino acid sequence able to specify nuclear location. *Cell* 1984;39:499-509.
  55. Cazalla D, Zhu J, Manche L, Huber E, Krainer AR, Caceres JF. Nuclear export and retention signals in the RS domain of SR proteins. *Mol Cell Biol* 2002;22:6871-82.
  56. Sapphire AC, Bark SJ, Gerace L. All four homochiral enantiomers of a nuclear localization sequence derived from c-Myc serve as functional import signals. *J Biol Chem* 1998;273:29764-9.
  57. Safran M, Kim WY, O'Connell F, Flippin L, Gunzler V, Horner JW, Depinho RA, Kaelin WG, Jr. Mouse model for noninvasive imaging of HIF prolyl hydroxylase activity: assessment of an oral agent that stimulates erythropoietin production. *Proc Natl Acad Sci U S A* 2006;103:105-10.
  58. Laemmli UK. Cleavage of structural proteins during the assembly of the head of bacteriophage T4. *Nature* 1970;227:680-5.
  59. Schagger H. Tricine-SDS-PAGE. *Nat Protoc* 2006;1:16-22.
  60. Voss M, Fukumori A, Kuhn PH, Kunzel U, Klier B, Grammer G, Haug-Kroper M, Kremmer E, Lichtenthaler SF, Steiner H, Schröder B, Haass C, Fluhrer R. Foamy Virus Envelope Protein Is a Substrate for Signal Peptide Peptidase-like 3 (SPPL3). *J Biol Chem* 2012;287:43401-9.
  61. Radons J, Faber V, Buhrmester H, Volker W, Horejsi V, Hasilik A. Stimulation of the biosynthesis of lactosamine repeats in glycoproteins in differentiating U937 cells and its suppression in the presence of NH<sub>4</sub>Cl. *Eur J Cell Biol* 1992;57:184-92.
  62. Geismann C, Grohmann F, Sebens S, Wirths G, Dreher A, Hasler R, Rosenstiel P, Hauser C, Egberts JH, Trauzold A, Schneider G, Sipos B, Zeissig S, Schreiber S, Schafer H, Arlt A. c-Rel is a critical mediator of NF-kappaB-dependent TRAIL resistance of pancreatic cancer cells. *Cell Death Dis* 2014;5:e1455.
  63. Bikoff EK, Huang LY, Episkopou V, van MJ, Germain RN, Robertson EJ. Defective major histocompatibility complex class II assembly, transport, peptide acquisition, and CD4+ T cell selection in mice lacking invariant chain expression. *J Exp Med* 1993;177:1699-712.
  64. Lutz MB, Kukutsch N, Ogilvie AL, Rossner S, Koch F, Romani N, Schuler G. An advanced culture method for generating large quantities of highly pure dendritic cells from mouse bone marrow. *J Immunol Methods* 1999;223:77-92.

## Figure Legends

**Figure 1: Gal4/VP16 assays are not applicable to SPPL2a/b substrates.** A) The 25 kDa Gal4/VP16 tag interferes with trafficking of murine TNF. For reporter assays based on Gal4/VP16 driven expression of a firefly luciferase a TNF construct was generated that harbored the Gal4/VP16 reporter at its N-terminus. HeLa cells seeded on coverslips were transiently transfected with HA-TNF-V5 or Gal4/VP16-TNF-V5 and the subcellular distribution of the TNF fusion proteins was analyzed by indirect immunofluorescence using an antibody against an N-terminal epitope of TNF. In parallel, endogenous GM130 was visualized. B) The Gal4/VP16-TNF fusion protein is not processed by SPPL2a. HeLa cells were transfected with either of the two TNF constructs alone or in combination with SPPL2a or the catalytically inactive SPPL2a D416A mutant (D/A). In order to inhibit endogenous SPPL2a, cells were treated for 6 h with the SPPL-inhibitor inhibitor X (1  $\mu$ M) as indicated. Total cell lysates were analyzed by Western blotting with an antibody against an N-terminal epitope detecting the TNF full-length protein as well as different NTFs derived from the HA- and Gal4/VP16-tagged TNF. C) Transcriptional activation induced by the Gal4/VP16-TNF-V5 construct does not depend on SPPL protease activity. HeLa cells were transiently transfected with Gal4/VP16-TNF-V5, a response plasmid with a firefly luciferase under the control of a Gal4-dependent promoter (pL8G5-Luc) and a constitutively expressed Renilla luciferase (pRL-TK). Cells were treated for 6 h with 1  $\mu$ M inhibitor X and processed for determination of firefly and Renilla luciferase activities. The normalized ratio of firefly/renilla activities is shown. Bars indicate mean values of n=4 experiments  $\pm$  SEM. One-way ANOVA with Tukey post hoc testing was performed. \*\*\*P<0.001; ns, not significant. D) An N-terminal GFP-tag disturbs subcellular trafficking of CD74. HeLa cells were transfected using CD74-HA or CD74 tagged with the 24 kDa GFP-tag at its N-terminus (GFP-CD74) and subsequently analyzed for the distribution of the expressed proteins by indirect immunofluorescence using the In-1 antibody directed against the N-terminus of CD74. Co-staining for endogenous PDI was performed. E) NTFs derived from GFP-tagged CD74 are not processed by SPPL2a. Processing of CD74-HA or GFP-CD74 was compared upon co-expression of both constructs with active or inactive (D/A) SPPL2a in transiently transfected HeLa cells. In B) and E)  $\beta$ -actin served as loading control.

**Figure 2: The  $\beta$ Gal  $\alpha$ -tag for  $\beta$ GEFC does not interfere with trafficking and processing of SPPL2a/b substrates.** A) Design of the  $\beta$ GEFC-assay for quantitative detection of the CD74 ICD after its liberation by intramembrane proteolysis. In endosomes, proteolytic processing of CD74 generates an N-terminal fragment (NTF) that is subjected to SPPL2a intramembrane cleavage. In the assay, a CD74 fusion protein with the N-terminally appended  $\beta$ Gal  $\alpha$ -peptide is expressed in a reporter cell line that stably expresses the catalytically inactive  $\beta$ Gal  $\omega$ -fragment localized to the nucleus. After proteolytic release, the CD74 ICD is released to the cytosol and able to traffic to the nucleus thereby restoring  $\beta$ Gal activity that serves as sensitive and quantitative readout. B) To test application of the small  $\alpha$ -tag to the SPPL2a substrate CD74 two constructs were designed that differed in the presence or absence of an extrinsically added NLS between the  $\beta$ Gal  $\alpha$ -peptide and the CD74 N-terminus. C) Endosomal/lysosomal targeting of CD74 was not impaired by the N-terminally appended  $\alpha$ -peptide. The subcellular localization of  $\alpha$ -CD74 and  $\alpha$ -NLS-CD74 in comparison to CD74 devoid of any N-terminal tag was analyzed by immunofluorescence using the In-1 antibody in transiently transfected HeLa cells. Co-localization with the lysosomal/late endosomal protein LAMP-2 was determined with the 2D5 antibody. Scale bars = 10  $\mu$ m. D) Processing of the different  $\alpha$ -tagged CD74 reporter constructs by co-expressed active, but not inactive (D/A) SPPL2a was evaluated by Western blot analysis of transiently transfected HEK293 cells stably expressing the  $\beta$ Gal  $\omega$ -fragment in the nucleus ( $\omega_{\text{nuc}}$  cells) in comparison to CD74 without any N-terminal tag. E) Proteolytic cleavage of the  $\alpha$ -tagged CD74 as expressed from the assay constructs by endogenous protease levels was validated by application of SPP/SPPL inhibitors to  $\omega_{\text{nuc}}$  cells transiently transfected with the indicated CD74 constructs. Cells were treated with inhibitor X (InX, 1  $\mu$ M) or (Z-LL)<sub>2</sub>-ketone (ZLL, 20  $\mu$ M) for 6 h prior to cell harvest.

**Figure 3: Establishment of a  $\beta$ GEFC assay to measure nuclear translocation.** A) Design of a galactosidase based reporter construct. The  $\omega_{\text{nuc}}$  reporter construct is based on *E. coli*  $\beta$ Gal with deletion of the  $\alpha$ -peptide (aa 12-42) resulting in a catalytically inactive  $\omega$ -fragment. Nuclear localization of the construct was enabled by addition of three SV40 nuclear localization sequences (NLS), a nuclear retention signal (NRS) from SC35 protein and a c-Myc-derived NLS. Nuclear transport of the reporter protein in a subcloned stable cell line was validated by indirect immunofluorescence analysis using an anti- $\beta$ Gal antibody. B) As a positive control with constitutive nuclear localization, an N-terminally  $\alpha$ -tagged eGFP-construct was designed by fusing the  $\beta$ Gal  $\alpha$ -tag and three NLS to the 5'-end of the eGFP-coding sequence. Fluorescence microscopy showed distinct  $\alpha$ -eGFP<sub>nuc</sub> expression in the nucleus in transiently transfected HeLa cells. C) As a negative control with a definite extranuclear localization, human TMEM192, an integral membrane protein of lysosomes with four transmembrane segments (TM), was tagged N-terminally with the  $\beta$ Gal  $\alpha$ -peptide and in addition with an HA epitope to enable detection. Presence of the fusion protein in lysosomes was validated in transiently transfected HeLa cells by indirect immunofluorescence by staining with the HA 3F10 antibody for TMEM192 and the 2D5 antibody for the lysosomal marker protein LAMP-2. Scale bars = 10  $\mu$ m (A-C). D) Functionality of the assay was validated by expression of the positive and negative control constructs (B,C) in the  $\omega_{\text{nuc}}$  reporter cell line characterized in A) and quantification of  $\beta$ Gal activity using a luminescent assay. The determined  $\beta$ Gal signal was divided by the value obtained for activity of the firefly luciferase (Luc) co-transfected with the assay constructs. The  $\beta$ Gal/Luc

ratios were normalized to the value from the  $\alpha$ -eGFP<sub>nuc</sub> positive control. Bars indicate mean values of n=3 experiments  $\pm$  SEM. One-way ANOVA with Tukey post hoc testing was performed. Significance versus vector-transfected cells is depicted. \*\*\*P<0.001, ns, not significant.

**Figure 4: Nuclear translocation of the CD74 ICD can be detected by  $\beta$ GEFC and is dependent on SPPL2a activity.** A) The  $\alpha$ -CD74 ICD is capable of entering the nucleus as shown by  $\beta$ GEFC assay in the  $\omega$ <sub>nuc</sub> reporter cell line.  $\beta$ Gal activity was determined in  $\omega$ <sub>nuc</sub> cells following transient transfection of  $\alpha$ -CD74 and  $\alpha$ -NLS-CD74 as well as the  $\alpha$ -eGFP<sub>nuc</sub> positive and the  $\alpha$ -TMEM192 negative controls. To account for differences in transfection activity,  $\beta$ Gal activity was normalized using firefly luciferase (Luc). The calculated  $\beta$ Gal/Luc ratios were further normalized to that of  $\alpha$ -eGFP<sub>nuc</sub> positive control. Bars indicate mean values of n=3 experiments  $\pm$  SEM. Significance of the CD74-expressing versus the  $\alpha$ -TMEM192 transfected cells is depicted. B) Dependency of the determined  $\beta$ Gal/Firefly Luciferase ratio on the amount of expressed CD74 was verified by transient transfection of different amounts of plasmids coding for  $\alpha$ -tagged CD74. Mean values were calculated from n=3 experiments and error bars indicate SEM. C) Co-transfection of SPPL2a with  $\alpha$ -CD74 increases the CD74-associated  $\beta$ Gal/Luc activity ratio. Upon concurrent inhibition of SPPL2a activity by application of inhibitor X (InX, 1  $\mu$ M, 6 h) this effect was abolished. Bars indicate mean values of n=3 experiments  $\pm$  SEM. D) Inhibition of endogenous SPPL2a by inhibitor X (InX, 1  $\mu$ M) or (Z-LL)<sub>2</sub>-ketone (ZLL, 20  $\mu$ M) for 6 h reduced the CD74-associated  $\beta$ Gal/Luc signal. A similar reduction of  $\beta$ Gal complementation in  $\omega$ <sub>nuc</sub> cells transiently transfected with  $\alpha$ -CD74 was observed upon interference with the activity of proteases involved in processing of the CD74 luminal domain. This was performed by application of bafilomycin A1 (300 nM), E-64 (10  $\mu$ M) or leupeptin (2.5  $\mu$ M). Bars indicate mean values of n=3-7 experiments  $\pm$  SEM. Significance of values from inhibitor-treated versus solvent-treated cells is depicted. E) Knock-down of SPPL2a in  $\omega$ <sub>nuc</sub> reporter cells reduced the normalized  $\beta$ Gal activity following expression of  $\alpha$ -CD74. Cells were transfected twice with non-targeting control siRNA or siRNA directed against SPPL2a prior to transfection with the  $\alpha$ -CD74 substrate construct. Reduction of cellular SPPL2a levels and an accumulation of the CD74 NTF were confirmed by Western blotting. Bars indicate mean values of n=3 experiments  $\pm$  SEM. For statistical analysis, one-way ANOVA with Tukey post hoc testing (A,C,D) or an unpaired, two-tailed Student's t test (E) was performed. \*\*\*P<0.001, \*\* P<0.01, \*P<0.05.

**Figure 5: The CD74 ICD is degraded by the proteasome and activates expression of *SFRP2*.** A) Incubation of  $\alpha$ -CD74 transfected  $\omega$ <sub>nuc</sub> cells with the proteasome inhibitors epoxomicin (1  $\mu$ M) and bortezomib (5  $\mu$ g/ml) clearly increased  $\beta$ Gal complementation while application of a cytosolic peptidase inhibitor mix (Ama/Best/AAF) of amastatin (1  $\mu$ M), bestatin (20  $\mu$ M) and AAF-CMK (10  $\mu$ M) had only minor effects. Bars indicate mean values of n=3 experiments  $\pm$  SEM. B) The effect of epoxomicin shown in A), could be partially blocked by inhibition of SPPL2a by preincubation with inhibitor X (1  $\mu$ M) respectively. Bars indicate mean values of n=4 experiments  $\pm$  SEM. One-way ANOVA with Tukey post hoc testing was performed. C) Application of the proteasomal inhibitors epoxomicin and bortezomib only has minimal effects on the  $\beta$ Gal  $\omega$ -fragment.  $\omega$ <sub>nuc</sub> cells were treated for 6 h with epoxomicin or bortezomib and subsequently analyzed for the stabilizing effect of these compounds on the reporter fragment by Western Blotting.  $\beta$ -actin served as loading control for normalization of densitometric quantification. D) Design of an inducible system for controlled overexpression of the CD74 ICD (aa 1-35). The ICD of CD74 was attached to a membrane anchored GFP by a TEV cleavage site or an uncleavable stretch of seven alanines (A<sub>7</sub>). Co-expression of a TEV protease via an IRES element only liberated the CD74 ICD in presence of the ENLYFQG cleavage site. The membrane-tethered cleavable (CD74-ICD-TEV-GFP<sub>mem</sub>) and non-cleavable (CD74-ICD-A<sub>7</sub>-GFP<sub>mem</sub>) CD74-ICD-GFP fusion proteins were expressed from the depicted constructs that were used for the generation of stable FlpIn<sup>TM</sup>-Rex<sup>TM</sup>293 cell lines. E) Characterization of the cell lines stably expressing CD74 ICD-TEV-GFP<sub>mem</sub> or CD74-ICD-A<sub>7</sub>-GFP<sub>mem</sub> upon induction with doxycyclin. FlpIn<sup>TM</sup>-Rex<sup>TM</sup>293 cell lines were generated based on the constructs shown in D) and treated with 10  $\mu$ g/ml doxycyclin for 24 h or left untreated. Expression of the fusion proteins was detected by Western blotting using anti-CD74 or anti-GFP antibodies. The TEV protease was visualized with anti-Myc. F) *SFRP2* is transcriptionally upregulated after overexpression and liberation of the CD74 ICD. The cell lines characterized in E) were treated for 24 h with 10  $\mu$ g/ml doxycyclin in order to induce expression of the CD74-ICD-GFP fusion proteins. *Secreted frizzled-related protein 2* (*SFRP2*) expression was determined by qRT-PCR in both cell lines and normalized for expression of tubulin. Normalized *SFRP2* transcript levels were significantly increased in the cell line expressing the cleavable CD74 ICD fusion protein (TEV) versus the control cell line (A<sub>7</sub>) where the ICD is not liberated. G) *Sfrp2* is downregulated in SPPL2a and CD74 deficient BMDCs compared to wildtype cells. For statistical analysis, one-way ANOVA with Tukey post hoc testing was performed. Significances in A) are depicted for inhibitor-treated versus solvent-treated cells. Also in B) significance of values from inhibitor-treated versus solvent-treated cells was depicted. Furthermore, significance of additional inhibitor X treatment in epoxomicin-treated cells was evaluated. In G) significances of SPPL2a or CD74 deficient versus wildtype BMDCs are indicated, lines mark significances between single conditions. \*\*\*P<0.001, \*\* P<0.01, \* P<0.05, ns, not significant.

**Figure 6: SPPL2-dependent nuclear translocation of the TNF and ITM2B ICDs.** A) To test further described SPPL2 substrates for nuclear translocation of their proteolytically liberated ICDs, assay constructs similar to those for CD74 were designed for TNF and ITM2B. In the ITM2B expression constructs also an HA-tag was added to allow antibody detection. B) The  $\alpha$ -tag does not interfere with sorting of ITM2B and TNF. Comparison of HA-tagged ITM2B and HA-TNF-V5 with the corresponding  $\alpha$ -tagged fusion proteins by indirect immunofluorescence revealed no major differences regarding the subcellular distributions of the proteins in HeLa cells. Expression of ITM2B was determined using the HA 3F10 antibody while TNF localization was detected with a rabbit polyclonal against the N-terminus of the protein. Scale bars = 10  $\mu$ m. C)  $\beta$ GEFC assays indicate nuclear translocation of TNF and ITM2B ICDs. Normalized  $\beta$ Gal activity was determined in  $\omega_{nuc}$  reporter cells transiently expressing the indicated constructs. Bars indicate mean values of n=3 experiments  $\pm$  SEM. D) Co-expression of active SPPL2a and SPPL2b enhanced the  $\beta$ GEFC assay signal in  $\alpha$ -TNF expressing  $\omega_{nuc}$  reporter cells. This effect of co-expressed SPPL2a/b was blocked by concurrent administration of inhibitor X (InX, 1  $\mu$ M) for 6 h. Bars indicate mean values of n=4-5 experiments  $\pm$  SEM. E) The assay signal induced by  $\alpha$ -ITM2B could also be augmented by overexpression of SPPL2b and SPPL2a. Experiments were carried out in analogy to  $\alpha$ -CD74 and  $\alpha$ -TNF before. Bars indicate mean values of n=3 experiments  $\pm$  SEM. One-way ANOVA with Tukey post hoc testing was performed. In A) significances versus the  $\alpha$ -TMEM192 transfected cells were depicted. In D) and E) significances for the effect of the SPPL2a/b overexpression alone or in combination with inhibitor X application are shown. \*\*\*P<0.001, \*P<0.05, ns, not significant.

**Figure 7: The devised  $\beta$ GEFC assay is also applicable to other I-CLIPs like  $\gamma$ -Secretase.** A) A Notch1 reporter construct for the  $\beta$ Gal assay was designed based on the Notch1 $\Delta$ E construct which lacks the extracellular portion of the Notch1 receptor. Therefore, the resulting protein is constitutively processed by  $\gamma$ -secretase to generate the Notch1 ICD (NICD) for which nuclear translocation is well documented. The employed construct exhibited the  $\beta$ Gal  $\alpha$ -peptide and an additional HA-tag at its C-terminus. B)  $\gamma$ -secretase inhibition prevented generation and nuclear translocation of the NICD and stabilized the uncleaved Notch $\Delta$ E- $\alpha$  protein at the plasma membrane. HeLa cells transiently expressing Notch $\Delta$ E- $\alpha$  were treated with 1  $\mu$ M DAPT for 6 h and analyzed by indirect immunofluorescence using the HA 3F10 antibody. C) Application of the  $\gamma$ -secretase inhibitor DAPT, but not the SPP/SPPL inhibitor (Z-LL)<sub>2</sub>-ketone (ZLL) reduced the normalized  $\beta$ Gal activity determined in the  $\omega_{nuc}$  reporter cell line following transient transfection of Notch $\Delta$ E- $\alpha$ . Post transfection, cells were incubated overnight and subsequently treated with DAPT (1  $\mu$ M), ZLL (20  $\mu$ M) or DMSO as vehicle control for 6 h. Bars indicate mean values of n=3 independent experiments  $\pm$  SEM. Scale bars = 10  $\mu$ m. One-way ANOVA with Tukey post hoc testing was performed. Significance of values from Notch $\Delta$ E- $\alpha$  expressing versus TMEM192 transfected cells and of the inhibitor treatments was depicted. \*\*\* P<0.001, ns, not significant.

## Supporting Information

Item	Associated with	Significance for the paper
Suppl. Table S1	Figure 5	Full list of differentially expressed genes from the microarray experiment, requested by reviewer
Suppl. Table S2	Figure 5	List of NFκB target genes from the microarray dataset. The data exclude a major NFκB activation as a reason for the <i>SFRP2</i> upregulation by the CD74 ICD. A statement on this was requested by one of the reviewers.
Suppl. Figure S1	Figure 5	Full experimental data on the validation of additional targets from the microarray experiments that were not followed up further, requested by reviewer.

**Suppl. Table S1: Full list of putative CD74 ICD target genes.** Microarray analysis of the inducible TREX CD74 ICD-TEV-GFP<sub>mem</sub> and CD74-ICD-A<sub>7</sub>-GFP<sub>mem</sub> cell lines was performed. The relative abundance of transcripts was determined and the fold change (TEV/A<sub>7</sub>) was calculated. The table comprises all identified targets with a fold change > 2.0 or < -2.0. Protein-coding transcripts are marked in red.

**Suppl. Table S2: NFκB target genes are not differentially regulated by the liberated CD74 ICD.** Gene expression profiles of the inducible TREX CD74 ICD-TEV-GFP<sub>mem</sub> and CD74-ICD-A<sub>7</sub>-GFP<sub>mem</sub> T-Rex™ were obtained by microarray analysis. The expression of documented NFκB target genes (<http://www.bu.edu/nf-kb/gene-resources/target-genes/>) as well as genes associated to the NFκB-signaling pathway (KEGG hsa04064) was compared based on the calculated fold change (TEV/A<sub>7</sub>). No significant effect that would support a significant impact of the liberated CD74 ICD on the NFκB pathway in this cell system was observed.

**Suppl. Figure S1: Validation of transcriptional targets identified in the microarray experiment.** The inducible TREX CD74 ICD-TEV-GFP<sub>mem</sub> and CD74-ICD-A<sub>7</sub>-GFP<sub>mem</sub> cell lines were treated for 24 h with 10 μg/ml doxycyclin in order to induce expression of the CD74-ICD-GFP fusion proteins. Expression of *TULP3*, *ZNF763*, *SFRP2*, *DHRX*, *LUM*, *TPTE* and *CNTN1* was determined by qRT-PCR in both cell lines and normalized for expression of tubulin. The following primers in addition to those specified in the Materials & Methods section were used:

hTULP3-fw, CCAGATAGTCCACAAAATGACC;	hTULP3-rv, GCCTGTACTGCACAAAGTGG;
hZNF763-fw, GCTGTGCCCTTCTGTAGTCA;	hZNF763-rv, CCACAGGGTCCTGAAACATC;
hDHRX-fw, CGGCTGGTTGCTTTTCAA;	hDHRX-rv, TCTCTTCTCGTTGTATAGGTAATGG;
hLUM-fw, GAAAGCAGTGTCAAGACAGTAAGG;	hLUM-rv, GGCCACTGGTACCACCAA;
hTPTE-fw, CCCCAGGCTCTTCTGACC;	hTPTE-rv, AGAATCTGGTAGTGAATCCATAACTCT;
hCNTN1-fw, GATGACTGGAAAGATGCAAAGA;	hCNTN1-rv, CATGGGATTAAGTCCACTGCT.

**Figure 1**

*Nuclear translocation after intramembrane cleavage*

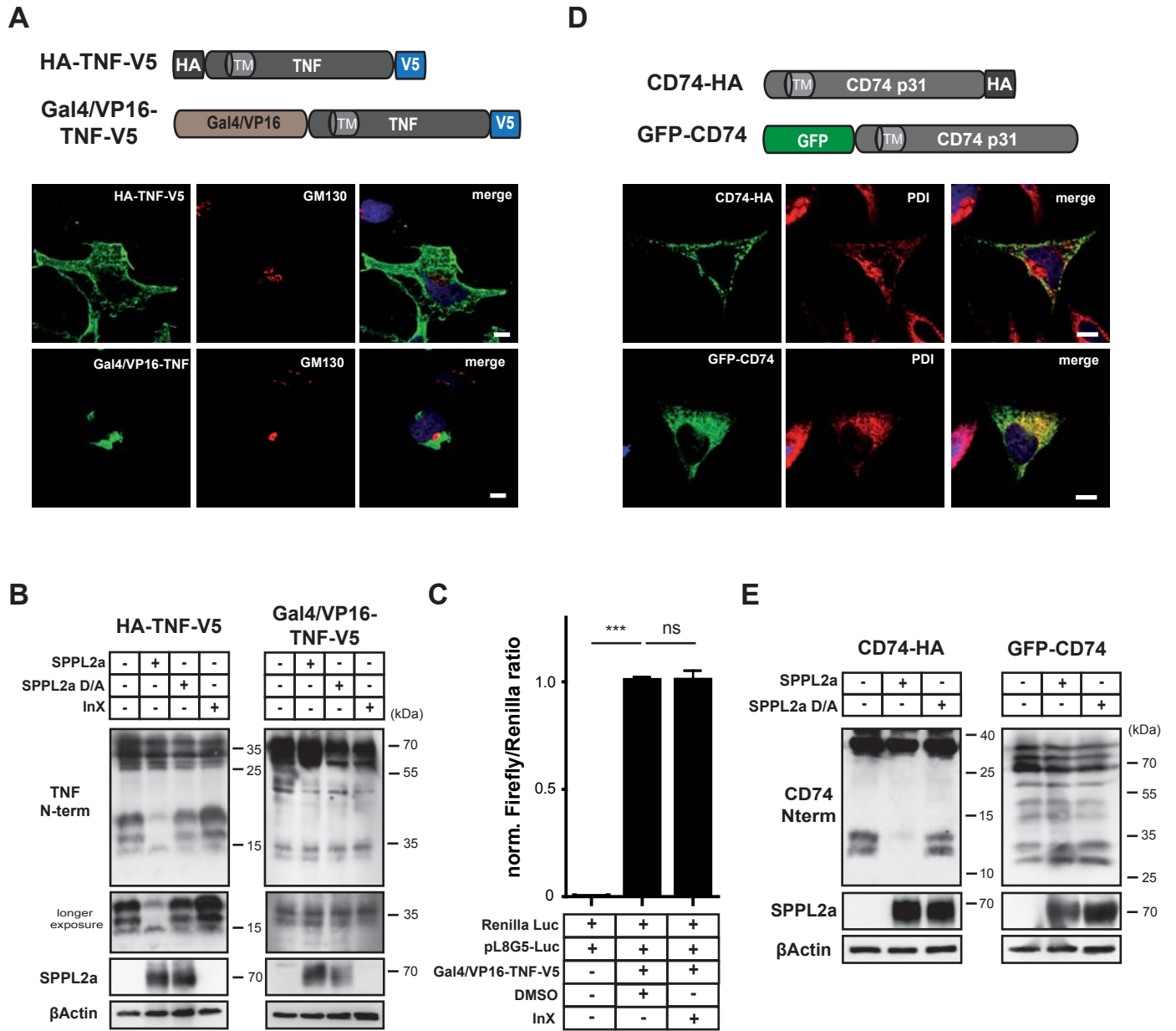


**Figure 2**

*Nuclear translocation after intramembrane cleavage*

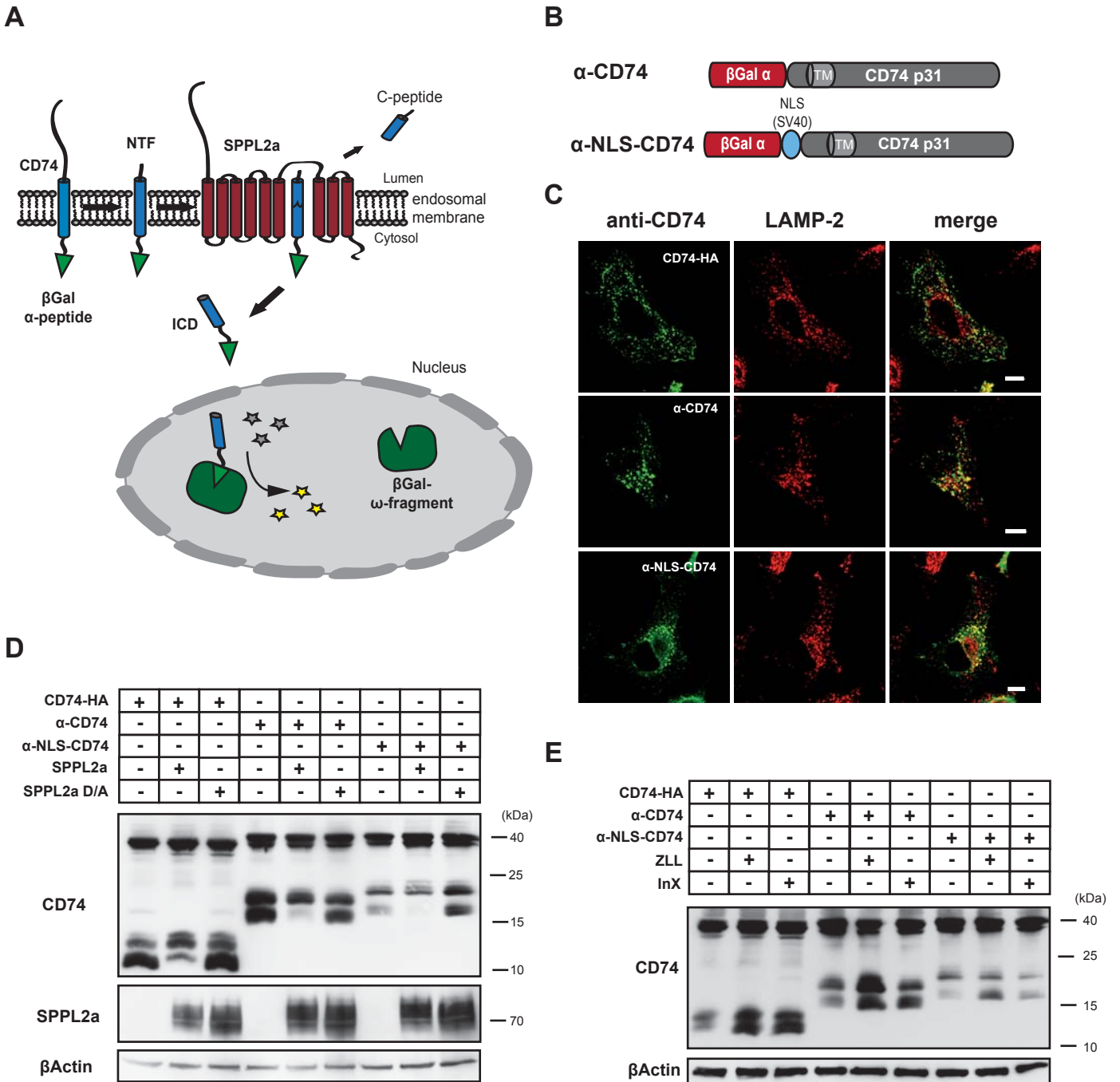


**Figure 3**

*Nuclear translocation after intramembrane cleavage*

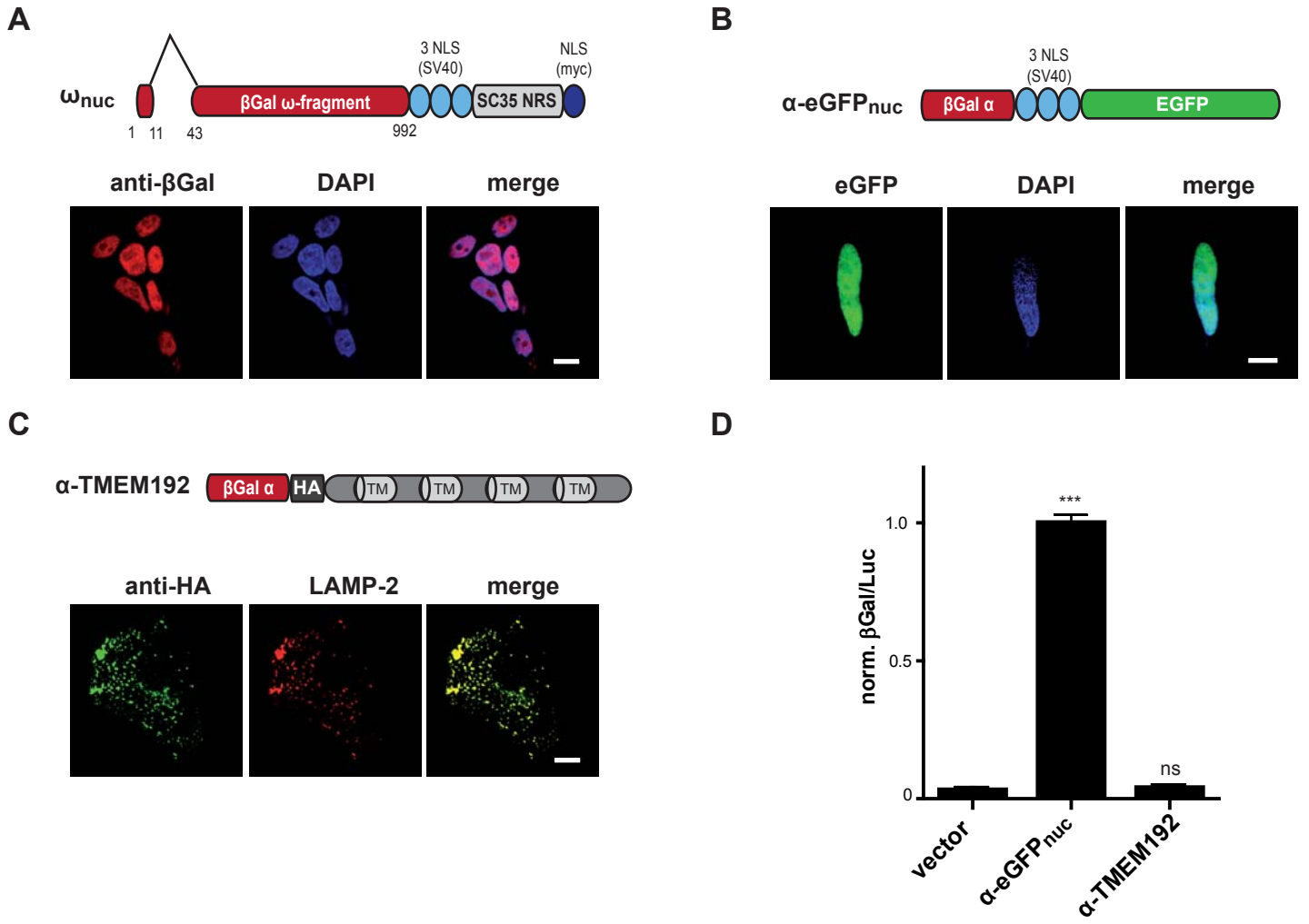


**Figure 4**

*Nuclear translocation after intramembrane cleavage*

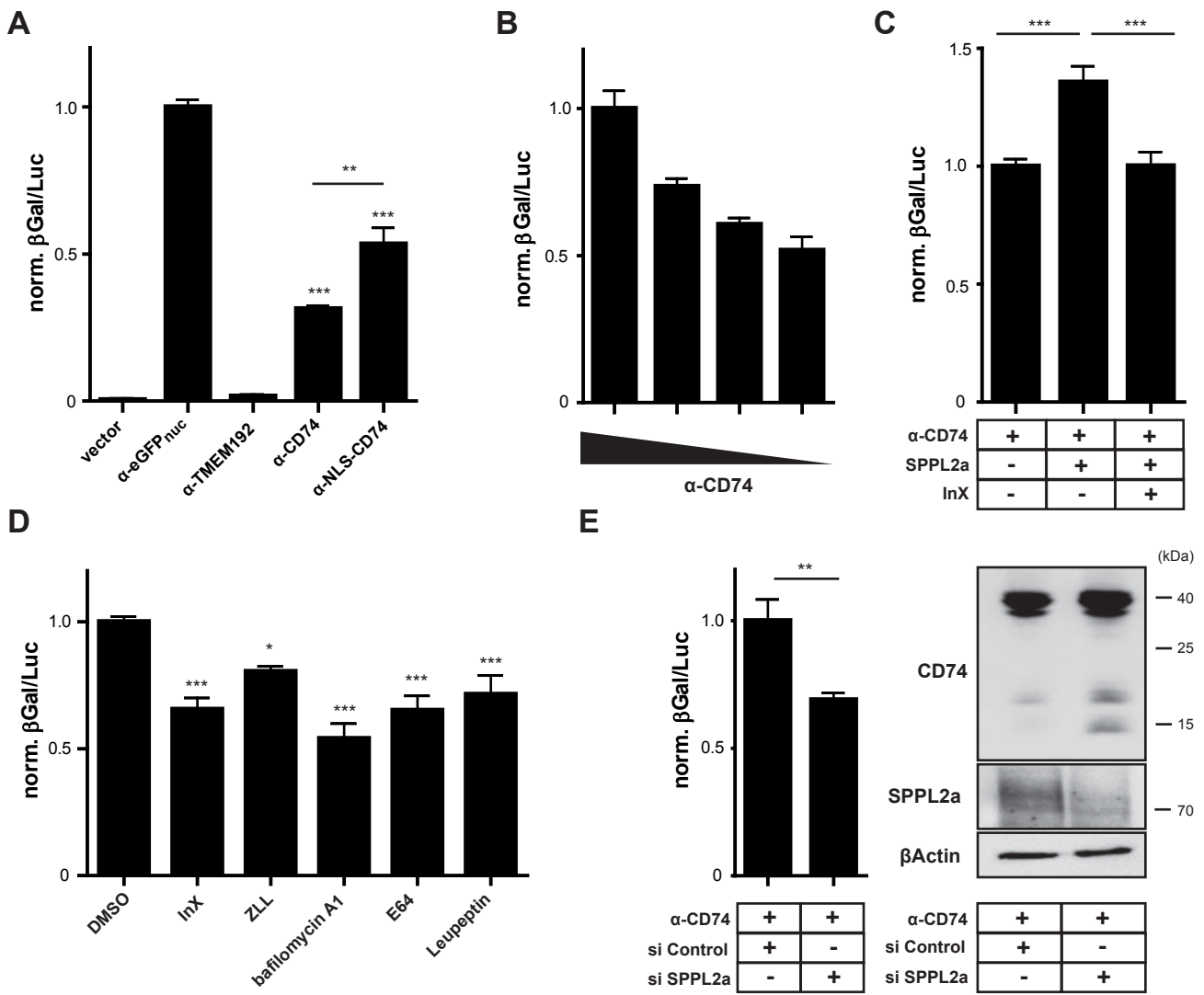


**Figure 5**

*Nuclear translocation after intramembrane cleavage*

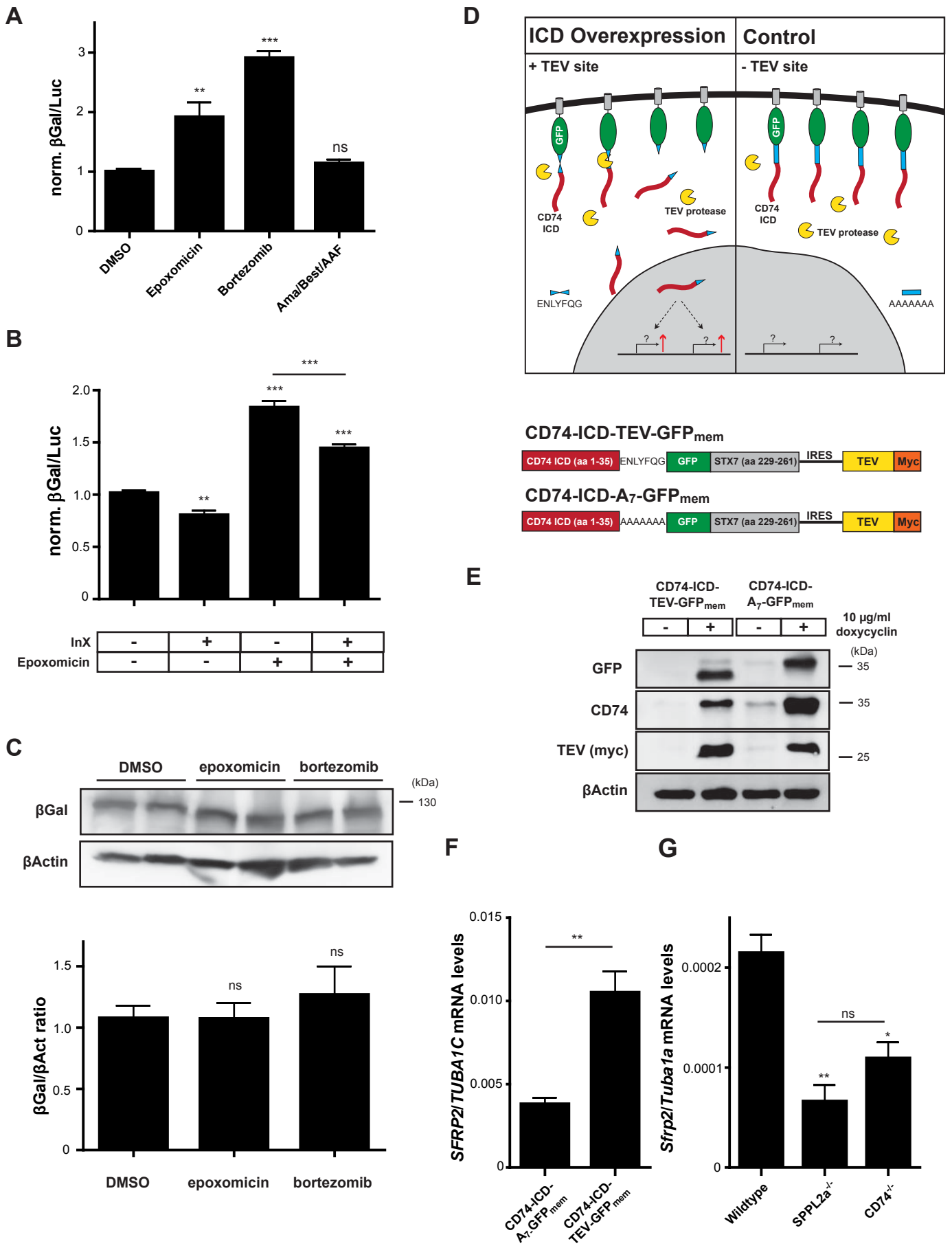


**Figure 6**

*Nuclear translocation after intramembrane cleavage*

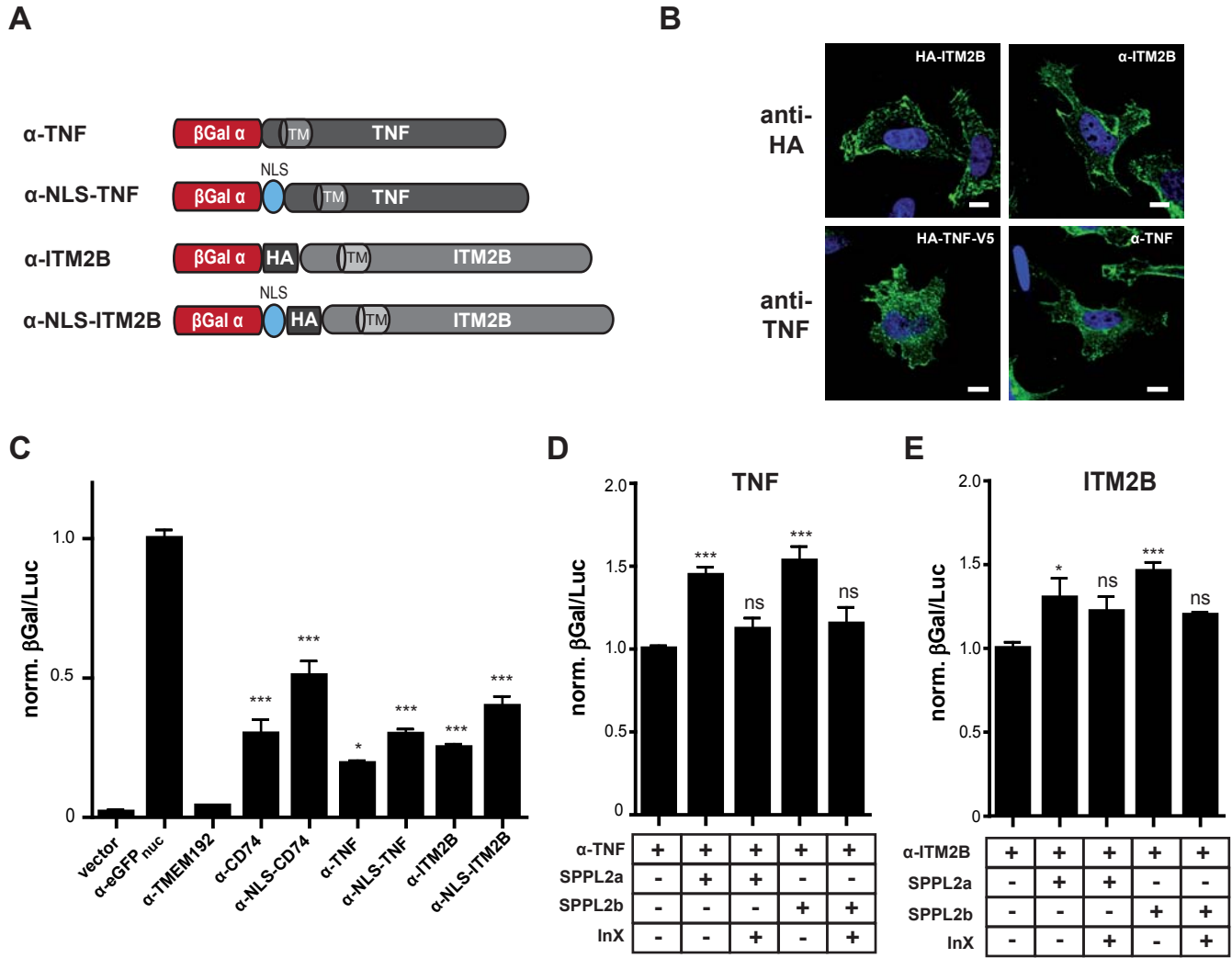
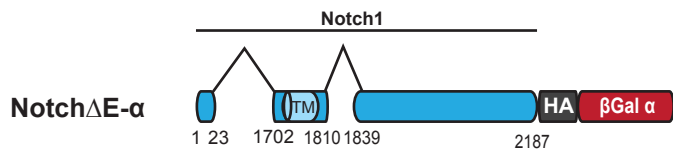


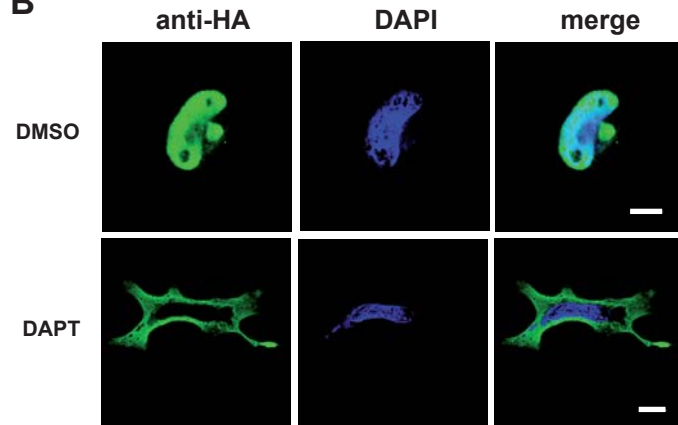
**Figure 7**

*Nuclear translocation after intramembrane cleavage*

**A**



**B**



**C**

